CHAPTER 6
FINITE ELEMENT MODEL OF A SOIL-BENTONITE CUTOFF WALL

6.1 Introduction

A finite element model of a soil-bentonite cutoff wall was developed for this research. The model simulates all stages of soil-bentonite cutoff wall construction, including excavation of the trench under a bentonite-water slurry, replacement of the bentonite-water slurry with soil-bentonite backfill, and consolidation of the soil-bentonite backfill. Deformations measured at the Raytheon site described in Chapter 5 indicate that most of the deformations in adjacent ground occurs after backfilling, and therefore it is important to include consolidation of the soil-bentonite in the model. The finite element program SAGE (Bentler et al. 1998), which was developed at Virginia Tech, was used for the analyses. SAGE has a fully coupled formulation for fluid flow and deformation, and is capable of modeling consolidation of the soil-bentonite as well as the other phases of construction. The RS constitutive model described in Chapter 4 was implemented in SAGE and was used to represent soil-bentonite. The finite element model was calibrated using the Raytheon case history. The lateral movements recorded from inclinometers at the Raytheon site, along with settlement data, were used to revise the procedures and material properties of the finite element model. Good agreement was achieved between the predicted and measured deformations for the revised model. After successful calibration of the model, it was used in a parametric study, which is described in Chapter 7.

In this chapter, previous examples of finite element modeling of soil-bentonite cutoff walls are reviewed first. Next, preliminary finite element studies with SAGE are described, including verification calibration of the RS model in SAGE and simulation of arching theory. Soil models and soil parameters used to represent the Raytheon site are described next, together with soil testing data from the site. A description of the finite element model is then given, and procedures used to model the construction sequence are described. The calculated deformations from the finite element model are compared to the measured deformations. The calibration of the model is described including the

effects of changing various parameters and procedures. A revised model is then compared with the measured deformations, and good agreement was achieved.

6.2 Previous Examples of Finite Element Modeling of Soil-Bentonite Cutoff Walls

Two examples of finite element modeling of soil-bentonite cutoff walls were found in the literature. Also, modeling of the soil-bentonite cutoff wall at the Raytheon site was performed by Harding Lawson Associates (HLA 1987b) in an unpublished study. These three examples are presented and evaluated in this section.

A finite element study described in *Barrier* (1995) was performed to model the consolidated stresses in soil-bentonite backfill in a completed soil-bentonite cutoff wall. The study is described as "imperfectly modeled," with the following drawbacks: 1) the finite element program could not simulate the excavation process, backfill process, or consolidation of the soil-bentonite backfill, 2) soil parameters for the native soils were not available, and 3) no method was used between soil-bentonite elements at the trench wall and elements of the native ground to allow sliding at the interface. Despite these drawbacks, the study indicates that vertical effective stresses in the center of the soil-bentonite cutoff wall are less than geostatic and close to stresses estimated from dilatometer testing that was performed in the completed wall.

The *Barrier* (1995) study does not simulate the complexities of soil-bentonite cutoff wall construction. Since details of the modeling procedures are not provided, they cannot be evaluated for usefulness or accuracy.

A second example of finite element modeling of a soil-bentonite cutoff wall was performed by Clark (1994). A soil-bentonite cutoff wall was to be constructed in existing ground, and a levee built on top of the cutoff. The objectives of the modeling were to study stress transfer during soil-bentonite consolidation and the potential for hydraulic fracturing of the soil-bentonite cutoff wall. Two studies were performed. All materials

were modeled with an elastic-plastic Mohr-Coulomb model that incorporated the following parameters: bulk modulus, shear modulus, friction angle, dilation angle, cohesion, and tensile strength. An interface element was used at the trench wall. The interface element parameters were shear stiffness, normal stiffness, friction, and cohesion. The model was interpreted to consist of the following stages: 1) initial stresses of existing soils were established using gravity forces and assuming K_o=0.5, 2) trench excavation was modeled by changing material parameters of the alluvial soils in the trench to properties of a bentonite-water slurry, 3) formation of a filter cake at the trench wall was modeled by changing the properties of the frictional interface, 4) backfilling with soil-bentonite was modeled by incrementally changing the properties of the slurry to the properties of the soil-bentonite. The analyses indicate that construction of the trench should result in negligible settlement or lateral deformations of the adjacent soil. The author concludes that "weak arches" develop in the upper 5 meters of the trench but that these will be "broken" by consolidation of the soil-bentonite, and that there is no significant reduction in stress in the soil-bentonite due to arching. In the second study by Clark (1994), only the trench is modeled and one-dimensional and two-dimensional consolidation of the soil-bentonite was studied. The trench walls were fixed in the lateral direction. Settlement magnitudes at various times are estimated for the different drainage conditions and different permeabilities.

In Clark's first study, changing the material properties in steps 2 and 4 above, does not accurately model the excavation of one material and replacement with another material. Excavation and fill placement cause changes in stress to adjacent elements, and if new materials are "wished in place" these changes are ignored. In addition, changing material properties to model backfilling assumes that the initial stress state in the soil-bentonite trench is the same as the geostatic conditions in the soil that it is replacing. This is not a good procedure, since the objective of the model was to study the stresses in the soil-bentonite. The findings from Clark's numerical studies do not agree with the observed trends in behavior for other cutoff walls presented in Chapter 2 and Chapter 5. Specifi-

cally, stresses in completed soil-bentonite cutoffs have been measured to be less than geostatic and significant ground deformations have been recorded due to soil-bentonite cutoff wall construction.

Clark's second study, in which the sides of the trenches were fixed laterally, models the time rate of deformation of a column of soil-bentonite, and provides no information on deformations in adjacent ground.

In an unpublished study, finite element modeling of the soil-bentonite cutoff wall at the Raytheon site was performed by Harding Lawson Associates (HLA 1987b). Ground settlements due to construction of the cutoff were estimated. The finite element program NESSI (Cundall et al. 1980) was used for the analysis. The program was described by HLA as follows: The program is for soil interaction of dynamic and static loading conditions. Soil deformation is assumed to consist of shear deformation and volume change. Shear deformation is controlled by the shear modulus, and a hyperbolic relationship between shear stress and shear strain is assumed. Volume change is controlled by a constant bulk modulus (or constant Poisson's ratio). The program does not handle pore-water pressure generation and dissipation.

The following procedure was used to estimate "short term" displacements due to excavation under bentonite-water slurry: 1) initial stress conditions were established assuming gravity loads, K_o values, and building loads, and 2) excavation under bentonite-water slurry was modeled. Details of this procedure are not provided but it was stated that stress changes were caused by a) stress relief in the trench due to excavation and b) the weight of the slurry.

Next, "long term" displacements were estimated. Long term displacements were assumed to be caused by the following mechanism. Excavation causes elements within a few feet of the trench to undergo tension, heave, water absorption, and volume expan-

sion. After wall installation, these soil elements undergo compression, pore pressure increase, and decrease in volume. This decrease in volume would cause ground displacements and settlement near the wall.

These "long term" displacements were estimated using the following procedure: 1) initial stress conditions were assumed to be the same as calculated in step 2 for "short term" displacements, 2) the trench is assumed to be full of soil-bentonite, and 3) Poisson's ratio of soil elements within a few feet of the wall was lowered to 0.2 to simulate consolidation due to pore pressure dissipation.

Settlement at an adjacent building at 490 Middlefield Road was estimated to be ½ inch after excavation and ¾ inch after consolidation of the soil-bentonite. The settlement at this building was measured as 0 to ½ inch after excavation and backfill and ½ to 4 inches after consolidation.

The analysis appears to employ reasonable procedures for the initial stress conditions and excavation phase. Good agreement between the predicted and measured settlement was achieved for the excavation phase. The procedures for backfilling are hard to evaluate based on the information given, and the mechanism and procedure for "long term" displacements does not appear reasonable. The analysis underpredicts the deformations after placement of the soil-bentonite backfill. The analysis appears to have the following limitations: 1) consolidation of the soil-bentonite was not considered to be a mechanism for deformations, 2) the finite element code was not able to predict pore pressure generation and dissipation, and 3) an unrealistic initial stress state was assumed for the soil-bentonite.

Conclusions

The three previous examples of finite element modeling of soil-bentonite cutoff walls described in this section show that it is difficult to accurately model the complex condi-

tions of soil-bentonite cutoff wall construction. It is important to accurately model excavation and backfilling of the trench and the corresponding changes in stress in the ground adjacent to the trench. These phases of construction cannot be accurately modeled by simply changing the material properties or material model. A realistic initial stress condition for the soil-bentonite as first placed in the trench must be assumed or calculated. In addition, it is important to model consolidation of the soil-bentonite after placement in the trench.

6.3 Preliminary Finite Element Analyses

Before the finite element model of a soil-bentonite cutoff wall was developed, preliminary finite element analyses were performed. These analyses are briefly described in this section and are detailed in Appendix B. The analyses include verification of the RS model in SAGE, and simulation of arching.

The RS constitutive model developed for representation of soil-bentonite was implemented into the finite element code SAGE and verified. The following loading conditions were simulated: axisymmetric drained compression, axisymmetric undrained compression, one-dimensional consolidation, isotropic consolidation, and plane strain compression. The finite element analyses were verified with other numerical or analytical methods and/or checked for reasonableness. The results of the RS verification indicate that the RS model in SAGE is consistent with the model's theory, and the model performs as intended in SAGE.

A finite element analysis to simulate arching theory in a soil-bentonite cutoff wall was performed. Arching theory is described in Section 2.3. The trench was 10 ft deep and 5 ft wide. The full width of the trench was modeled. The trench walls were fixed in the lateral direction, as assumed in arching theory. Five columns of 2-D elements were used for the soil-bentonite backfill in the trench. Interface elements were used at the trench walls to represent the filter cake. The RS model was used for the soil-bentonite and

properties from soil-bentonite mixture SB1 were used. An interface element, which is described in the SAGE manual and uses an elastic hyperbolic relationship between shear stress and displacement, was employed in the analyses. Properties for the interface were obtained from direct shear tests on filter cakes performed by Laura Henry, who was a graduate research assistant at Virginia Tech at the time (Henry et al. 1998). Plots of shear stress versus displacement were used to find property values that provided a good fit to the results of tests that were run at four different normal stresses.

The soil-bentonite backfill was assumed to be in place in the trench with an assumed initial stress state. The initial effective vertical stress was assumed to be very low and constant with depth. Excess pore pressures were assigned equal to the total weight of the soil-bentonite minus the initial vertical effective stress. Initial horizontal effective stresses were assumed to be equal to the vertical effective stresses. The excess pore pressures were allowed to dissipate with time during the analyses. The results indicate the following: a) over time, the pore pressures dissipate and reach hydrostatic conditions, b) vertical effective stresses in the center of the trench approximate stresses calculated using arching theory, and c) the trend of settlement in the trench approximates the trend corresponding to arching theory, i.e. there is very little deformation at the trench walls and the most settlement occurs in the center of the trench. The analyses show that arching theory can be simulated using finite element analyses with SAGE, and that dissipation of initial excess pore pressures in the soil-bentonite backfill can be modeled.

6.4 Modeling Soil Conditions at Raytheon

For finite element modeling of the soil-bentonite cutoff wall at Raytheon, material parameter values were developed for the native soil, soil-bentonite, bentonite-water slurry, and filter cake. As described in Chapter 5, soil conditions at Raytheon consist of a complex system of layered coarse and fine grained soils. A representative soil profile, shown in Figure 6.1, was developed to represent the conditions along the southern leg of the cutoff wall, where most of the instrumentation was located. The profile consists of an

upper clay layer and alternating lower layers of sand and clay. The profile is based on 12 borings that were taken along the southern leg of the wall. The average depth of water was estimated to be 15 ft at the site. This depth was used to interpret the soil testing and laboratory data. A water level of 17.7 ft was measured in piezometers near the southern leg of the cutoff wall just before construction of the cutoff. This depth of water was used in the finite element modeling to represent the initial ground water condition. The depths of the borings used to create the soil profile range from 100-180 ft in depth with the majority of the borings terminating around 165 to 170 ft, typically in CL material. Borings were terminated in the layer described in project documentation as the B/C aquitard. The aquitard is estimated to extend to depths of 200 to 250 ft.

The Duncan and Chang (1970) hyperbolic model, described in Section 4.3, was used to model the sand. The Modified Cam Clay model, described in Section 4.4, was used to model the clays. The RS model, described in Section 4.6, was used to model the soil-bentonite. The bentonite-water slurry was modeled with an equivalent fluid pressure.

It was originally intended to model the filter cake using interface elements along the side of the trench wall. The intent was to use the elastic interface model that worked well for arching analyses as discussed in the previous section. Unfortunately, these interface elements did not perform well with the finite element model that was developed for full analysis of the soil-bentonite cutoff wall. Problems were encountered after excavation and filling of the interface elements. This is described in more detail later in this chapter after a discussion of backfill modeling procedures.

Instead of an interface element, a very thin 2-D element of soil-bentonite was used at the trench wall. Half of the width of the trench was modeled, and three columns of 2-D elements of soil-bentonite were used to represent the half-width, with the very thin element next to the trench wall. Related research on filter cakes sheared in direct shear tests indicated that the effective stress strength parameters were $c'=0$ and $\phi'=32$ degrees

(Henry et al. 1998). The strength of the filter cakes at Raytheon was assumed to be the same, and was modeled with a thin 2-D element of soil-bentonite that has ϕ'=32 and c'=0. In this way, the strength of the filter cake was accounted for in the modeling. One element problems were run with SAGE on a thin 2-D soil-bentonite element to observe the deformation behavior of long, thin elements. It was found that thin elements with aspect ratios of 1:20 were well behaved in shear, and showed reasonable stress-strain behavior. Details of the one element problem are in Appendix B.

The hydraulic conductivity of the filter cake was modeled by "smearing" the hydraulic conductivity of the filter cake into the element of soil adjacent to the trench. The hydraulic conductivity of the elements next to the trench were lowered to account for the lower hydraulic conductivity of the filter cake. The procedure is described in more detail at the end of this section.

Geotechnical data from laboratory tests, field tests, and in situ tests was compiled from the following reports:

1) Golder Associates (1987). "Interim Remedial Measures, Raytheon Semiconductor Division, Mountain View, California, Vol. I and Vol. II." March 1987, Redmond, Wash.
2) Harding Lawson Associates (1987a). "Soil Mechanics Laboratory Tests for Slurry Trench Cutoff Wall, 350 Ellis Street Site, Mountain View, CA." February 3, 1987, revised March 20, 1987, Novato, CA.
3) Harding Lawson Associates (1987b). "Ground Deformation Analysis, Slurry Cutoff Wall Installation, Raytheon Building Sites, Mountain View, CA." April 27, 1987, San Francisco, CA.
4) Harding Lawson Associates (1989). "Ground Deformation Analysis, Slurry Cutoff Wall, Raytheon Facility, Mountain View, CA." August 18,1989, San Francisco, CA.
5) Trautwein. "Test Program for a Soil-Bentonite Slurry obtained from the GKN Hayward Baker – Raytheon Site in Mountain View, CA."

From this data, model parameter values were interpreted. The parameter values for all materials used in the finite element model are listed in Table 6.1.

Sand Parameter Values

The unit weight of the sand was estimated from unit weight or water content data for five samples of SC, SM, or GP materials (USCS classification) at various depths. SPT N values or equivalent SPT values are plotted in Figure 6.2. Only tests performed in sands are plotted. Most sampling at the site was performed with a 3 inch O.D. sampler with a 200 lb hammer and 18 inch drop or a 140 lb hammer and 30 inch drop. The N values with the oversized sampler were converted to equivalent SPT N values using a procedure described by Pond (1996). Pond achieved good correlations with SPT and oversized samplers with this method in sands and gravelly sands. Average N values were chosen for each sand layer and converted to N_1 values using a conversion factor by Seed et al. (1985). The average N_1 value for each sand layer ranges from 59-55. Various correlations for sand with averaged N_1 values indicate friction angles between 38-56 degrees (McGregor and Duncan 1998).

The values of the strength parameters c' and ϕ' for the sand were estimated from two CU tests, one staged CD test, and correlations with SPT N values. The CU tests indicate that c'=0 and ϕ'=37 degrees. The CD test, performed with three stages, indicates that c'=0 and ϕ'=45 degrees. A value of c'=0 and ϕ'=40 degrees was used in the analyses.

The hyperbolic parameter values of K_m, R_f, and n were found from the staged CD test. The parameter values of K_b and m could not be evaluated from the CD test since volumetric data was not reported. The parameter values of K_b and m were estimated from published values in Duncan et al. (1980) from similar sands. K_{ur} was assumed to be 1.2 times K, which is recommended for stiff soils (Duncan et al 1980). The K_o value was assumed to be the same as that estimated for the clay, which is discussed below. Tensile strength was assumed to be zero.

Table 6.1 Soil Parameter Values used in Finite Element Model

(a) Hyperbolic Model Parameter Values

Parameter	Sand
Total Unit Weight (pcf)	125
K_o	0.6
Cohesion (psf)	0
Friction Angle (degrees)	40
Tensile Strength (psf)	0
R_f	0.8
K	1000
K_{ur}	1200
n	0.6
K_b	750
m	0.2

(b) Modified Cam Clay or RS Model Parameter Values

Parameter	Upper Clay	Lower Clay	Soil-Bentonite
Total Unit Weight (pcf)	125	125	118
K_o	1.2	0.6	0.6
M	1.37	1.37	1.3
κ	0.005	0.005	0.005
λ	0.091	0.091	0.071
Poisson's ratio	0.42	0.42	0.35
N (for pressure in psf)	2.46	2.46	2.12
R	NA	NA	2.01
S	NA	NA	2.01

(c) Bentonite-Water Slurry Data

Parameter	Bentonite-Water Slurry
Total Unit Weight (pcf)	74

(d) Hydraulic Conductivity Data

Material	k (cm/s)
Sand	1.0×10^{-4}
Sand Smear	1.1×10^{-7}
Upper Clay	5.0×10^{-7}
Upper Clay Smear	9.2×10^{-8}
Lower Clay	5.0×10^{-7}
Lower Clay Smear	9.2×10^{-8}
Soil-Bentonite	1.0×10^{-8}
Filter Cake	3.0×10^{-9}

Clay Parameter Values

The unit weight for the clays was estimated from the average of 41 samples of CL, ML, or CL-ML material, according to USCS. The average unit weight was 123 pcf, and a value of 125 pcf was used in the analyses. SPT N values or equivalent SPT N values are plotted in Figure 6.3 for penetration tests performed in clayey samples. The same procedures used for the sands were also used to estimate average N and average N_1 values for each clay layer. N_1 values range from 20 to 48 and generally increase with depth. An N_1 value of 24 was estimated for the upper clay layer and an N_1 value of 48 was estimated for the lowest clay layer.

Liquid limit and plastic limits tests were run on 49 samples of clayey material. The average liquid limit is 38 and the average plasticity index is 16, which classifies the average clayey material as CL according to USCS. 70% of the samples classify as CL, 10% classify as ML, 4% classify as CL-ML, and 4% classify as CH according to USCS.

Effective stress strength parameters were interpreted from 16 CU tests from various reports. The maximum principal stress ratio was chosen as the failure criterion. The tests indicate a linear failure envelope with c'=0 and ϕ'=34 degrees. The value of M is 1.37 using equation 3.7, which relates ϕ' to M.

The overconsolidation ratio for each clay layer was interpreted from 14 one-dimensional consolidation tests performed on samples taken from various depths. The preconsolidation pressure, p_p, from each test is shown in Figure 6.4, as indicated by the open circles. Also shown is the vertical effective stress, σ_y', assuming geostatic stress conditions, as indicated by a solid line. A representative p_p profile was estimated, as indicated by a dashed line. Average preconsolidation pressures were estimated for each clay layer and OCR values were calculated for the middle of each layer. The OCR values were used to estimate the lateral earth pressure coefficient, $K_{o,}$ from the following equation by Mayne and Kulhawy (1982).

$$K_o = (1 - \sin\phi')\,OCR^{\sin\phi'} \qquad (6.1)$$

The friction angle of 34 degrees found from the CU tests was used in the above equation. The estimated stress history of each clay layer is shown in Table 6.2.

Table 6.2 Stress History of Clay Layers

Mid-Depth of Clay Layer	σ_y' (ksf)	p_p' (ksf)	OCR	p_p'- σ_y'	K_o
6.5	0.8	5.0	6.2	4.2	1.2
38.5	3.3	7.0	2.1	3.6	0.7
58.5	4.6	7.7	1.7	3.1	0.6
79.5	5.9	8.7	1.5	2.8	0.6
97.5	7.0	10.0	1.4	3.0	0.5
121	8.5	11.2	1.3	2.7	0.5
168	11.4	13.5	1.2	2.1	0.5

A K_o value of 1.2 was used to model the upper clay layer and a K_o value of 0.6 was used to model the lower clay layers. According to the values in Table 6.2, the preconsolidation pressure is 2.1 to 4.2 ksf greater than the overburden pressure. The overconsolidation profile was approximated in the finite element analyses by applying and then removing a surcharge of 3.2 ksf to the entire site.

The Modified Cam Clay compressibility parameter values of λ, κ, and N, were found from 1-D consolidation tests. Representative values of λ and κ were chosen from the slopes of virgin compression and recompression curves respectively, giving more weight to higher quality tests. The value of N was estimated by plotting void ratio versus mean consolidation pressure for the normally consolidated portions of the 1-D consolidation tests and the isotropically consolidated CU tests, and estimating the location of the isotropic consolidation line. The mean consolidation pressure was estimated from the 1-D consolidation tests using an average K_o value of 0.6.

Poisson's ratio was estimated using the procedure described in Section 4.3. This procedure uses the shear modulus estimated from CU tests at various mean effective stresses.

The value of Poisson's ratio is calculated from the definition of bulk modulus for the Modified Cam Clay model and the model's compressibility relationships.

Values of undrained strength with depth were compiled but were not used in the finite element analyses, since effective strength parameters were used. The undrained shear strengths from CU tests, UU tests, and unconfined compression tests on clays are shown in Figure 6.5.

Soil-Bentonite Parameters

The unit weight of the soil-bentonite was found from the average of 243 tests performed by the engineer and contractor during construction. Other tests on soil-bentonite that were performed frequently for QA/QC purposes include slump, bentonite content, and percent fines. The number of tests performed were 261, 149, and 66 respectively. The average values for the soil-bentonite are: slump= 4.5 inches, bentonite content= 2%, and percent fines= 53%. Four water content tests were performed on soil-bentonite samples, with an average value of 31.9%.

Effective stress strength parameter values were interpreted from three CU tests on soil-bentonite. A value of $c'=0$ and $\phi'=32$ degrees was used, which is the same strength value measured for the soil-bentonite mixtures (SB1 and SB3) used in the laboratory testing program. Stress-strain plots of the soil-bentonite at the site are similar in shape to plots of normally consolidated samples of SB1.

The value of Poisson's ratio was estimated from the initial portions of the CU tests as described in Section 4.3. The Poisson's ratio value was similar to the value found for SB1.

The RS Model compressibility parameter values of λ, κ, and N, were found from two 1-D consolidation tests. The value of λ was estimated from the slope of the normally consoli-

dated compression curve. Since no unload data was available from the tests, κ was estimated by correlating values of κ versus % fines, and κ/λ versus % fines, from SB1, SB3, and the clay at Raytheon. The value of N was found by plotting the estimated mean effective stress versus void ratio from 1-D consolidation tests assuming a K_o value of 0.6. The value of K_o was assumed, based on the measured value of K_o=0.57 for SB1, since the soil-bentonite at Raytheon has compressibility properties and Atterberg limit values that are similar to SB1.

As described in Sections 4.5 and 4.6, the R parameter value can be estimated from CU tests and the S parameter value can be estimated from CD tests. CD tests were not performed on the soil-bentonite, so it was not possible to estimate the S parameter value from site specific laboratory data. However, the value of S was found to be the same for both SB1 and SB3, and this value (S=2) was assumed for the soil-bentonite at Raytheon. The R parameter value was estimated by adjusting the parameter value to find the best fit with three CU tests. A value of R=2 was found to be the best fit with the CU data. The fitting procedure involved use of a spreadsheet program developed for constitutive modeling studies as part of this research. The estimated values of M, λ, κ, ν', and N discussed above were used with the appropriate confining pressure to model each CU test. The predictions of the RS model from the spreadsheet with R=2 and S=2 are shown in Figure 6.6 with the CU test data. It can be seen in the figure that a good fit was found using these parameter values and the RS Model.

Since the R and S values were both estimated to be 2 for the soil-bentonite, the Modified Cam Clay model could have been used instead of the RS Model. As described in Section 4.6, the RS model is the same as the Modified Cam Clay model with R and S values equal to 2. For the RS Model as implemented in SAGE, a value of 2.01 was used instead of 2.0, because numerical instabilities result if the R or S values equal exactly 2. During verification of the RS Model in SAGE, the RS Model was verified to produce the same

results for a variety of loading conditions as the Modified Cam Clay model if the R and S values equal 2.01.

Bentonite-Water Slurry Properties

The average unit weight of the in-trench bentonite-water slurry was found to be 74 pcf from 443 unit weight tests. The slurry was modeled using an equivalent fluid pressure against the sides and the bottom of the trench.

Hydraulic Conductivity Values

The hydraulic conductivity of the sand layers was determined from in situ and laboratory tests. Many pump tests and slug tests were run on different sand layers, which are referred to in the project documents as the A, B1, B2, and B3 aquifers. These aquifers are described in Section 5.2. The results of all the in situ hydraulic conductivity tests that were performed in the aquifers are plotted versus the aquifer mid-depth in Figure 6.7 as triangles. The tests indicate that all of the aquifers have similar hydraulic conductivity values, although the values exhibit considerable scatter, ranging from $1x10^{-4}$ to $1x10^{-1}$ cm/sec. The average value of these tests is $1x10^{-2}$ cm/sec. It is believed that this value is too heavily influenced by the larger values of hydraulic conductivity due to the large range of values. The median value of these tests is $7x10^{-3}$ cm/sec, which may be more representative of the range of values. Falling head hydraulic conductivity tests were also performed in the laboratory on sands classified as SC. These results are plotted in Figure 6.7 as squares, and are 1 to 6 orders of magnitude less than the field test results. The pump tests and slug tests were performed in bore holes, which were sand packed over a depth of 12 to 36 ft. These tests would be most influenced by the layers within these depths with the highest hydraulic conductivity value, and they also reflect the horizontal hydraulic conductivity of the sands. The laboratory tests were performed on samples a few inches in diameter, and they reflect the vertical hydraulic conductivity of the sands, which may be controlled by the presence of thin layers of clay or silt. A value of $1x10^{-4}$

cm/sec was chosen to represent the hydraulic conductivity of the sands, which is in-between the field and laboratory test values.

Falling head hydraulic conductivity tests were performed on 30 clayey samples, which were classified as CL or ML according to USCS. The results are plotted in Figure 6.7 as circles. The values of hydraulic conductivity generally range from $1x10^{-8}$ to $5x10^{-6}$ cm/sec. The median value of the tests is $8x10^{-8}$cm/sec. A larger value of $5x10^{-7}$ cm/sec was used because it is known that layers of sand exist within the clay layers.

The hydraulic conductivity of the soil-bentonite was estimated from 194 hydraulic conductivity tests by the contractor, engineer, and an independent consultant, as shown in Figure 6.8. The average value of the tests is $2x10^{-8}$cm/sec. The median value of $1x10^{-8}$ cm/sec was used in analyses. The measured hydraulic conductivity values were all lower than the specified maximum hydraulic conductivity of $1x10^{-7}$ cm/sec.

Laboratory test data from a related research project on filter cakes was used to estimate the hydraulic conductivity of the filter cake. The data indicate that for an average formation head of 50 ft, the permeability of the filter cake would be about 3 x 10^{-9} cm/sec (Henry et al. 1998). The permeability of the filter cake was modeled by "smearing" the hydraulic conductivity of the filter cake into the element of soil adjacent to the trench wall. The hydraulic conductivity of the adjacent element was reduced to reflect the lower hydraulic conductivity of the filter cake using the following equation:

$$k_{smear} = \frac{d_1 + d_2}{\frac{d_1}{k_1} + \frac{d_2}{k_2}} \qquad (6.2)$$

where: d_1=width of filter cake

d_2=width of adjacent element

k_1=hydraulic conductivity of filter cake

k_2=hydraulic conductivity of adjacent element

The equation is obtained by replacing a layered system consisting of the filter cake and adjacent element with an equivalent homogeneous system with flow perpendicular to the layering. Hydraulic conductivity of the "smear" elements were calculated for clay and sand elements adjacent to the trench and below the trench. The width of the filter cake was estimated to be 0.25 inch, based on the thickness of filter cakes measured in the laboratory (Adams et al. 1997). The resulting hydraulic conductivity values for the "smear" elements are listed in Table 6.1.

6.5 Description of the Finite Element Model

The finite element program SAGE was used to model the construction process of the soil-bentonite cutoff wall at the Raytheon site. The case history is described in detail in Chapter 5. A 2-D plane strain analyses was assumed, which simulates the 2-D nature of soil-bentonite cutoff walls and the long sections of trench that were used at the site. The section analyzed, which is shown in Figure 6.9, is at the southern leg of the cutoff wall at the location of inclinometer RGI-3. The native ground inside the cutoff and the half-width of the cutoff wall were modeled.

The program capabilities of SAGE are described in detail in the users manual (Bentler et al. 1998). The following capabilities that were used in the analyses of soil-bentonite cutoff walls for this research are briefly described below:

1) Coupled analysis: SAGE can perform fully coupled deformation and pore fluid flow analyses. This is necessary to model the consolidation of soil-bentonite.
2) Non-linear soil behavior: Newton-Raphson iteration is used in SAGE to solve the non-linear finite element equations arising from non-linear soil models. Several parameters are required to control the iteration solution process and specify convergence criteria.
3) Application of residual forces: SAGE uses construction steps to simulate loading of soil-structure systems. Each construction step is divided into a specified number of substeps. The applied force vector is applied incrementally over each substep and the

finite element equations are solved for each substep. SAGE has the option to apply residual forces (out-of-balance forces) from the end of one substep to the force vector of the next substep. This option was used for all analyses to prevent errors due to the incremental analysis process from accumulating.

4) Excavation of 2-D elements: A system of equal and opposite stresses is applied to the excavation boundary to produce a stress-free surface.
5) Placement of 2-D elements as fill: Gravity loads and buoyant forces are applied to the new elements. Pore pressures are not generated due to soil deformation due to placement, and displacements of newly placed nodes are set to zero at the end of the placement step. Piezometric lines are used to assign initial pore pressures in recently placed 2-D fill elements.

Input files were generated by hand with a spreadsheet and a mesh generation program. The output file was reduced with utility finite element programs developed by David Bentler while he was a research assistant at Virginia Tech. The reduced output was analyzed with graphing programs.

The mesh used in all analyses of the Raytheon site is shown in Figure 6.10, together with the boundary conditions used. The mesh represents a section of soil 200 ft deep by 580 ft wide. Recommendations from the literature for modeling an excavation with finite elements suggest that the mesh should extend to a depth where a relatively hard material is encountered (Dunlop and Duncan 1970; Kulhawy 1977). For the soil conditions at Raytheon, the clay N_1 values increase with depth and, to the depth explored, there is no clear boundary with a harder layer. The N values and N_1 values for penetration tests performed in the clay are shown in Figure 6.3. The consistency of the clay transitions from very stiff (N between 15-30) to hard (N>30), according to definitions from Terzaghi and Peck (1948). It was decided to terminate the mesh 100 ft below the bottom of the soil-bentonite cutoff wall, modeling approximately 100 ft of the hard clay. Recommendations from the literature for modeling an excavation also suggest that the mesh should

extend laterally a distance away from the excavation equal to three times the depth of the mesh (Dunlop and Duncan 1970; Kulhawy 1977). Three times the depth of mesh shown in Figure 6.10 would be 600 ft. This recommendation was almost achieved by modeling 580 ft laterally. The size of the mesh was limited by the maximum number of elements available with SAGE, and the desire to limit computational time.

The mesh shown in Figure 6.10 consists of 592 elements and 1883 nodes. Quadrilateral 2-D elements that have 8-displacement nodes and 4-corner pore pressure nodes where used. The average computational time on a personal computer with a 200 MHz Pentium Processor with 64MB RAM was 6 hours. A close up of the finite element mesh in the region of the soil-bentonite cutoff wall is shown in Figure 6.11. Three columns of elements were used to simulate the half-width of the soil-bentonite trench.

Roller boundary conditions were assumed at the sides of the mesh, i.e. the nodes were constrained in the x direction. The nodes were pinned along the bottom of the mesh, constraining the nodes in the x and y directions. A constant head boundary condition was maintained along the right boundary of the mesh. This head condition was varied according to the water elevation measured inside the area contained by the cutoff wall near the southern leg of the wall. The water elevations shown in Figure 5.11 were used. A temporary drawdown of approximately 6 ft was measured inside the area contained by the cutoff wall due to limited pumping. The model simulated this temporary drawdown measured inside the area contained by the cutoff wall, and because the model assumes symmetry on both sides of the cutoff wall, the drawdown occurs on both sides of the wall in the model. As shown in Figure 5.11, water levels outside the area contained by the cutoff wall increased temporarily by approximately 2 ft. The symmetric model neglects the temporary differential water pressure across the cutoff that is caused by drawdown of the water level in the area inside of the cutoff wall. It was estimated that the temporary differential water pressure is small (0 to 500 psf) in comparison to the excess pore pressures in the soil-bentonite after backfilling (1200 to 3200 psf) as calculated by the

model. Again, the assumption of symmetry on both sides of the cutoff wall was necessary to limit the size of the mesh and the computational time.

6.6 Procedures for Modeling Construction Sequence

The initial site conditions and construction process was modeled with the sequence of construction steps listed in Table 6.3. The input data file is in Appendix C.

Table 6.3 Steps for Modeling Construction Sequence

Sequence	Time for Each Sequence (days)	Time for Each Step (days)	Step Numbers	Total Head Boundary Condition (ft)
Assign initial stresses	NA	NA	-4	NA
Apply surcharge	NA	NA	-3	NA
Remove surcharge	NA	NA	-2	NA
Reassign horizontal effective stresses	NA	NA	-1	NA
Apply building loads	NA	NA	0	NA
Apply head boundary conditions	0.2	0.2	1	182.3
Excavate trench under bentonite-water slurry	8	8	2	182.3
Consolidation only	14	14	3	182.3
Backfill trench, replacing bentonite-water slurry with soil-bentonite	20	1.05	4-10	181.3
		1.05	11-22	180.3
Consolidation only	730	17	23	178.3
		36	24	177.4
		72	25	179.3
		72	26	182.0
		168	27	182.3
		365	28	182.3

Fully coupled fluid flow and deformation analyses were performed for steps 1 through 28. Steps before and including step 0 are used to establish initial site conditions in SAGE, and are uncoupled. A temporary drawdown of the water levels inside the area contained by the soil-bentonite cutoff wall was modeled by changing the total head

boundary condition at the right side of the finite element mesh as shown in Table 6.3. The bottom of the finite element mesh, which is 200 ft in depth, was taken as the datum for the head.

Initial Conditions

Steps –4 through 1 were used to establish the initial site conditions at the site, i.e., before construction of the soil-bentonite cutoff wall. Initial effective stresses were first assigned to the existing sands and clays using the unit weights and assuming geostatic conditions. A depth of water equal to 17.7 ft was assumed in the analyses for the initial condition. Although an average water table at 15 ft was measured over the site, the depth of water at the analyzed section was measured at 17.7 ft in the months prior to construction.

It was found that when performing coupled consolidation analyses with SAGE, if the water table is below the ground surface, the program calculates negative pore water pressures above the water table. The coupled consolidation option that was used (IG-CON=1), assumes that the pore fluid is incompressible and the soil is completely saturated with water. Over time, elements above the water table develop negative pore water pressures and eventually reach a steady state condition equal to:

$$u = \gamma_w z \qquad (6.3)$$

where:

u = pore pressure

γ_w = unit weight of water

z = depth below water table (negative values if above water table)

Several options were considered to try to avoid negative pore pressures above the water table since they are not usually assumed in practice, although they may exist due to capillary rise. The option in SAGE for coupled analyses with compressible fluid (IG-CON = -1) was tried. This option assumes that the fluid compressibility is a function of

the saturation of the soil and that the soil can be partially saturated. This option would not run and was not used.

Non-consolidating impermeable elements were considered for use above the water table. These elements have zero permeability and, during a coupled analysis, do not have any nodal head degrees of freedom. Pore pressures can be assigned to these elements using a piezometric line. These elements were not used since elements of soil-bentonite above the water table would not be able to dissipate excess pore pressures laterally into the adjacent soil.

It was only possible to model the dissipation of pore pressures from the soil-bentonite into the adjacent soils by assuming that negative pores pressures existed or would eventually develop above the water table. It was decided to assume that negative pore pressure above the water table existed as the initial condition, so that deformations would not be caused as a result of negative pore pressures eventually developing. The initial pore pressures assigned to the sand and clay in step -4 are shown in Figure 6.12. Although not a typical assumption, the assumption of negative pore pressures in the upper clay layer and sand above the water table is not unreasonable due to capillary rise. Typical height of capillary rise in clay soils has been estimated at greater than 32.8 ft, and typical height of capillary rise in a dense sand has been estimated at between 0.1 to 11.5 ft, depending on the grain size (Holtz and Kovacs 1981).

Initial vertical effective stresses were assigned at each node assuming geostatic stresses with the pore pressures shown in Figure 6.12. Horizontal effective stresses were calculated assuming a K_o value of 0.36 for the entire profile, which represents a normally consolidated condition in step –4.

As mentioned in Section 6.5, the results of many 1-D consolidation tests on clay samples indicate that the site is overconsolidated with the preconsolidation pressure was greater

than the overburden pressure over most of the depth by an average value of about 3200 psf. By applying a uniform surcharge pressure of 3200 psf in step –3 and then removing the surcharge in step –2, the OCR profile measured at the site was closely approximated. After removal of the surcharge, it was found that the horizontal effective stresses were unrealistically low, and so the horizontal effective stresses were then reset to equal K_o times the vertical effective stress in step –1. Values of K_o from Table 6.1 were used in step -1.

After preloading the site, the loads from the building at 350 Ellis Street were added to the mesh in step 0. The only information available on building loads were slides of an adjacent building at 490 Middlefield road. The building loads were estimated with the help of Professor Barker, a structural engineering professor at Virginia Tech. A load of 2300 psf was estimated for the load bearing exterior walls, and interior column loads combined with live load were estimated to be 150 psf. Since 350 Ellis street and 490 Middlefield road were both used for light industrial activity, and no further information was available, the same loads were used for the building at 350 Ellis street. SAGE considers the end of step 0 as the starting stress state, meaning that displacements and strains are measured from the end of step 0.

Head boundary conditions were applied in step 1, the first step with coupled flow analysis, to complete the modeling of the initial site conditions. The head boundary conditions in step 1 are consistent with the assigned initial pore pressures and did not cause any deformations or consolidation.

Excavation of Trench under Bentonite-Water Slurry

The excavation of the trench under bentonite-water slurry was modeled in step 2 by excavating the elements of sand and clay in the trench and applying stress distributions to represent the fluid pressure. Stress distributions were applied along the side of the trench and along the bottom of the trench equal to the unit weight of the slurry times the depth

of the slurry, as indicated in Figure 6.13. Research on stability of slurry filled trenches has shown that it is important to use the in-trench unit weight for the slurry (Adams et al. 1997). Also, the in-trench unit weight can be significantly higher than freshly prepared slurry due to suspended particles in the slurry. The in-trench unit weight of 74 pcf was used in these analyses.

The presence of the bentonite-water slurry was modeled only with fluid pressure because research on bentonite-water slurries has shown that the shear strength of bentonite-water slurry is very small and less than 1 psf (Adams et al. 1997). Therefore, the strength of the bentonite-water slurry is not significant for stability or strength considerations. It was also found through laboratory testing that penetration of bentonite-water slurry into granular soil caused no significant change in the shear strength of the granular soil (Adams et al. 1997).

During excavation, a filter cake is assumed to form along the trench wall as described in Section 2.2. The permeability of the filter cake was modeled by smearing the permeability of the filter cake into elements adjacent to the trench as described in the previous section. The filter cake was applied during the excavation step by lowering the permeability of the elements immediately adjacent to the trench and below the trench.

After excavation, the trench remained open, filled with bentonite-water slurry, for 14 days at the location of RGI-3. This was simulated by allowing 14 days of consolidation between excavation and backfilling in step 3.

Backfilling of Trench with Soil-Bentonite

To simulate the backfilling of the trench with soil-bentonite, elements of soil-bentonite were placed one row a time starting from the bottom of the trench. As each row of soil-bentonite was placed, the stress distributions representing the bentonite-water slurry were adjusted to reflect the replacement of the bentonite-water slurry with the soil-bentonite

backfill. The difficult part of this process was to estimate and then achieve the proper initial stress state in each recently placed row of soil-bentonite elements.

The stress state of soil-bentonite recently introduced in the trench has not been measured to date; however, it was approximated from the water content of the soil-bentonite about to be introduced into the trench and stress-strain information from 1-D consolidation tests. The initial water content of the soil-bentonite was measured to be 31.9%. Using the following equation, the void ratio of newly placed soil-bentonite was estimated:

$$G_s\, w = S\, e \qquad (6.4)$$

where:

G_s = specific gravity of solids

w = water content

S = degree of saturation

e = void ratio

The specific gravity of solids of the soil-bentonite was measured to be 2.7 and the degree of saturation was assumed to be 100%. Using equation 6.4, a void ratio of 0.86 was estimated for soil-bentonite being introduced into the trench. Two 1-D consolidation tests on the soil-bentonite were used to generate a plot of void ratio versus mean effective stress, by assuming a K_o value of 0.6, as shown in Figure 6.14. The mean effective stress was used because, as was shown in Chapter 3, void ratio has a unique relationship with mean effective stress for soil-bentonite. The isotropic consolidation line (icl) assumed with the RS model is also shown in Figure 6.14. It was assumed that soil-bentonite that has just slid into the trench is in a state of isotropic stress. The mean effective stress predicted by the isotropic consolidation line for a void ratio of 0.86 is 40 psf. This was estimated to be the initial stress state of soil-bentonite just entering the trench.

In SAGE, the initial stress of recently placed elements are calculated from the finite element method. The unit weight of the fill is used to calculate gravity loads and initial pore pressures are used to calculate buoyant forces. Initial pore pressures are specified

with the use of a piezometric line. Pore pressures are calculated based on the distance below the piezometric line and a specified unit weight of water. In SAGE, an elastic soil model is assumed for the element during the fill placement step. For 2-D elements, a Young's modulus equal to atmospheric pressure is assumed, and a Poisson's ratio, ν', is calculated from equation 6.5, where K_o is specified in the material properties section of the data input file.

$$\nu' = \frac{K_o}{(1 + K_o)} \tag{6.5}$$

A simplified analysis was used in order to establish the desired initial pore pressures in recently placed soil-bentonite elements. First, the stresses in a row of recently placed soil-bentonite elements was estimated, assuming that little or no shear stresses develop as a result of placement of the elements. Then, the desired height of the piezometric line was calculated in order to produce the desired initial effective vertical stress, σ_y', of 40 psf. A schematic of a recently placed row of soil-bentonite elements is shown in Figure 6.15. Using the dimensions defined in Figure 6.15, the total vertical stress, σ_y, and the pore pressure, u, at the mid-height of a row of soil-bentonite elements can be calculated from equations 6.6 and 6.7. The total vertical stress is due to the weight of the soil-bentonite and the pressure from the bentonite-water slurry above it. A height for the piezometric line was calculated, using equation 6.8, to produce a vertical effective stress, σ_y', equal to 40 psf in the middle of the row.

$$\sigma_y = \gamma_s h_s + \frac{h}{2}\gamma_{sb} \tag{6.6}$$

$$u = h_w \gamma_w \tag{6.7}$$

$$h_w = \frac{\gamma_s h_s + \frac{h}{2}\gamma_{sb} - \sigma_y'}{\gamma_w} \tag{6.8}$$

where:

γ_s = unit weight of slurry

γ_{sb} = unit weight of soil-bentonite

γ_w = unit weight of water for piezometric line

h_s = height of slurry above the top of soil-bentonite elements

h = height of soil-bentonite elements

h_w = height of piezometric line above mid-height of soil-bentonite elements

In order to achieve an initial vertical effective stress that was essentially uniform throughout the element, a unit weight of water, γ_w, almost equal to the unit weight of the soil-bentonite, γ_{sb}, was assigned to the piezometric line for the recently placed fill elements. The measured unit weight of the soil-bentonite is 118.0 pcf, and the unit weight of water assigned to the piezometric line for recently placed elements was 117.5 pcf.

As an example, the first row of soil-bentonite elements placed was 4 ft in height. After placement of the soil-bentonite, a height of 96 ft of bentonite-water slurry remains above the soil-bentonite. Using the following unit weights, γ_s=74 pcf, γ_{sb}=118 pcf, γ_w=117.5 pcf, and the following heights, h_s=96 ft, h=4 ft, the height of the piezometric line h_w is 62.128 ft (above the center of the element) from equation 6.8. Since the unit weight of water is close to the unit weight of the soil-bentonite, the vertical effective stress at the top of the element is 39 psf, and the vertical effective stress at the bottom of the element is 41 psf.

In summary, the height of the piezometric line was calculated to establish pore pressures that would give the desired initial effective stress at the center of the elements. A "heavy" unit weight of water was used to have essentially the same vertical effective stress throughout the depth of the element.

It was found that with the elastic soil model assumed by SAGE for elements being filled, recently placed soil-bentonite elements did not have the desired initial stress state. The initial vertical stress was much lower than the desired initial stress state in the first placed row, and in subsequently placed rows, σ_y' was negative. Initial vertical effective stresses were also not constant in the row of elements. It is believed that compression of the

elements occurred during placement, and relatively large shear stresses developed in the fill elements due to an assigned modulus value that was too large. Although a Poisson's ratio near 0.5 was used for fill elements to simulate an incompressible material, for numerical reasons, the maximum allowable value Poisson's ratio in SAGE is 0.498. This allows for finite compression of the elements during fill. Changes were made to SAGE by Dave Bentler in order to be able to specify a desired material model and material parameters that would be used for filled elements during the fill placement step. It was found that by using an elastic model with a very low Young's modulus and a Poisson's ratio value of 0.498, the desired initial effective stress in each row of recently placed soil-bentonite element could be achieved.

It was also found that if the height of the row of soil-bentonite was too high, or too many rows of soil-bentonite were placed in one step, the initial effective stresses would be too low. Stresses would also be different across the row of soil-bentonite, and would also be different for each row. From the results of small scale trench analyses, it was found that fill should be placed with a maximum height to width ratio of 5:1 to achieve the desired stresses with consistency across the row and for each subsequently placed row.

The material properties used for soil-bentonite during fill steps are summarized in Table 6.4.

Table 6.4 Modeling of Soil-Bentonite During Fill Placement

Soil Model	Initial σ_y' (psf)	Unit Weight (pcf)	Young's Modulus (psf)	Poisson's Ratio
Linear Elastic	40	118.0	0.01	0.498

Although the process described above was successful for placement of 2-D soil-bentonite elements, the process did not work for the placement of interface elements. Negative normal stresses were calculated in the interface elements even with reduced stiffness values for the interface. Many small scale and one element problems were run in order to

obtain positive and reasonable initial stresses in the interface, but with no success. Although some errors in SAGE were identified in this process and corrected by Dave Bentler, it appears that there is a problem with excavation and fill of interface elements using coupled analyses in SAGE. After placing an interface element, effective normal stress was not in equilibrium with the adjacent elements. Specifically, for a vertical interface element at the side of the trench, the effective normal stress was not equal to the effective horizontal stress in the adjacent soil-bentonite element. The issue could not be resolved, and interface elements were not used in the finite element model for this reason.

Consolidation of Soil-Bentonite

Excess pore pressures in the soil-bentonite that existed after the backfill process, were allowed to dissipate with time in steps 23 through 28. A time of 2 years after backfill placement was modeled in these steps. Figure 6.16 shows the average pore pressures in the soil-bentonite backfill in the column of elements closest to the centerline of the trench. The pore pressures calculated by the finite element model just after backfilling are shown with a dashed line. The final or steady state pore pressure distribution is shown by the solid line. The negative pore pressures that are assumed for the model are shown above a depth of 17.7 ft. Two years after backfilling, the pore pressures were hydrostatic and equal to the applied head boundary conditions at the right side of the mesh.

6.7 Comparison of Predicted and Measured Deformations

The predicted deformations from the finite element model were compared to the measured deformations. Measured deformations include lateral deformations from two inclinometers (RGI-2 and RGI-3), and settlement from various settlement points. The locations of the instrumentation are shown in Figure 6.9.

Incremental Lateral Deformation of Adjacent Ground

There are two inclinometers at the site that provide useful information for all phases of construction of the cutoff wall. One inclinometer, RGI-2 is located 12 ft from the center-line of the trench, and is on the outside of the area enclosed by the cutoff wall. One inclinometer, RGI-3, is located 28 ft from the centerline of the trench, and is on the inside of the area enclosed by the cutoff wall.

Inclinometer readings from RGI-3 were primarily used to calibrate the model. The finite element model simulates all phases of construction that occurred near RGI-3, including excavation, backfilling, consolidation, and a temporary drawdown of water levels that was recorded near RGI-3. Deformations at RGI-2 were also used to observe the range of lateral deformations that were recorded at the site. It should be kept in mind that RGI-2 is closer to the cutoff wall than RGI-3, and no drawdown occurred outside the area contained by the cutoff wall, where RGI-2 is located. In addition, deformations at RGI-2 indicate an abrupt displacement at a depth of 85 ft that developed during consolidation. This mechanism was not predicted by the finite element model and perhaps is due to a localized thin or weak layer.

The results of the finite element model are compared to readings at inclinometers RGI-2 and RGI-3 in Figure 6.17. Deformations from the finite element model at a distance of 27 ft from the trench centerline are plotted. The incremental lateral movement with depth is plotted for excavation, backfilling, and consolidation. Negative incremental deforma-tion is defined as movement toward the trench centerline. It is helpful to look at incre-mental deformations for lateral displacement since each phase of construction sets a new baseline reading for the next phase. In this way, adjustments could be made to the modeling process and material parameters during calibration to model each phase as closely as possible.

One thing to note about Figure 6.17 is that the shape of the lateral deformations with depth is similar for the inclinometer readings and the SAGE analysis. Both the measured and predicted deformations show that maximum lateral deformations occur at or near the ground surface and deformations gradually decrease with depth. Both the measured and predicted deformations show that very little incremental deformation (less than 1/4 inch) occurs below the cutoff wall at 100 ft depth. Also, the trend of movement is the same for both measured and predicted deformations for each phase. Specifically, they all show inward deformation during excavation, outward or no deformation during backfilling, and inward deformation during consolidation.

Since the shapes of the deformation versus depth plots are similar for both measured and predicted deformations, only the maximum incremental deformations for each construction phase are compared in the following discussion. Also, since it appears that the top 10 ft of the inclinometer casing of RGI-3 may have been bent or damaged, the maximum lateral deformation for RGI-3 is taken as the deformation at a depth of 10 ft. The inclinometers show a maximum inward lateral movement of about 1/4 to 1/2 inch after excavation of the trench. The finite element model predicts a maximum of about 1 1/2 inches of inward deformation. For the backfilling phase, the inclinometers show 0 to 1/4 inch of maximum outward lateral deformation. The finite element model predicts a maximum of about 1 1/4 inch of outward lateral deformation. For consolidation of the soil-bentonite, RGI-3 shows a maximum of 1 1/4 inch of inward movement. RGI-2 shows a maximum of 3/4 inch inward movement; however, it appears that most of this movement is a lateral translation from a potential slip surface at a depth of 85 ft. The finite element model predicts a maximum movement of about 1 3/4 inch for the consolidation phase. The finite element model shows the correct trend of movement for each phase of construction; however, the model overestimates the magnitude of lateral movement for each phase.

Total Settlement of Adjacent Ground

Data were available on two settlement points located inside the area contained by the cutoff wall, and six settlement points located outside the area contained by the cutoff wall. The total settlement versus distance from the trench centerline is plotted in Figure 6.18 for each construction phase. For most settlement points, data were only available for total settlement after consolidation of the cutoff wall; readings were not available for settlement during the excavation and backfilling phases. For this reason, the total settlement is plotted for each construction phase, and not the incremental settlement. The predicted total settlement from the finite element model is also plotted in Figure 6.18.

The settlement point data indicate that little settlement occurred after excavation and backfilling. Settlement points outside the area contained by the cutoff wall, which were within 20 ft from the wall, indicated 0 to 1/4 inch of heave after excavation and 0 to 1/4 inch of settlement after backfilling. The finite element model predicts a maximum of 1 3/4 inch of settlement after excavation and 1/2 inch of total settlement after backfilling.

After consolidation, data from settlement points were available at several distances from the trench. The data indicate that settlement decreases with distance from the trench, a trend also predicted by the finite element model. Again, it should be noted that the settlement points outside the area contained by the cutoff wall experience higher ground water levels than the settlement points inside the area contained by the cutoff wall, and higher than the ground water levels in the finite element model. Although higher groundwater levels would tend to decrease settlements, settlement points outside the area contained by the cutoff wall in general show greater settlement than the points inside. This indicates a wide range of values, which could be caused by differences in backfill properties, differences in construction procedures, or heterogeneity of soil conditions along the length of the trench. The data indicate a range of settlement from 1/2 inch to 3 1/2 inches at a distance of 20 ft from the trench. The finite element model predicts a maximum of 2 1/2 inches of settlement.

In general, the finite element model overpredicts the amount of settlement measured during excavation. The finite element model prediction of total settlement after the backfilling is close to measured values; however, the model predicts a significant amount of incremental heave during backfilling, which was not measured in the field. The finite element model overpredicts the majority of settlement points during the consolidation phase.

6.8 Calibration of Model and Results of Revised Analysis

During calibration of the finite element model, modifications to the procedures and material properties were investigated in order to obtain better agreement between predicted and measured movements. Changes were desired to decrease the amount of lateral movement during excavation and backfilling phases, and to slightly decrease the lateral movement during the consolidation phase. Similar trends were desired for settlement. Some modifications to the model resulted in better predictions of one phase of construction but worse predictions of another phase of construction. Some adjustments to material properties resulted in better predictions, but were ruled out as unrealistic assumptions. Eventually, two modifications were adopted to create a revised analysis, which had much better predictions of the ground deformations. These changes also seemed to be realistic. In this section, the effect of various modifications to the finite element model on adjacent ground deformations are described. The modified analysis is described, along with a comparison of the modified analysis results with the measured deformations.

Modifications to the Finite Element Model

Since the finite element model predicts similar trends for the lateral deformation and the settlement of adjacent ground, only the effect on lateral deformations will be described in this section.

It was found that reducing the initial K_o value of the existing sand and clay (during step -1) from 1.2 and 0.6 to 0.36 greatly reduced the amount of lateral deformation during excavation. This change had little effect on lateral deformations during backfilling and consolidation. Since the initial K_o values were based upon data from extensive 1-D consolidation tests with depth and the correlation from Mayne and Kulhawy (1982), there was reasonably good confidence in the estimated K_o values. It was felt that it would not be realistic to adjust the K_o values to this extent. The 1-D consolidation tests indicated an overconsolidated soil profile with OCR decreasing with depth. Assuming a K_o value of 0.36 would only be appropriate for a normally consolidated soil profile.

It was thought that perhaps the hydraulic conductivity of the existing clay and sand was overestimated, and during the times required for excavation and backfilling, an essentially undrained condition may exist, which may result in less deformations. The hydraulic conductivity of the existing clay and sand was greatly reduced; however, this did not cause a significant reduction in movements during excavation and backfilling.

In order to produce a stiffer response during excavation and backfilling, the stiffness of the sand was increased during loading and unloading-reloading. K was varied from 500 to 3000 and K_{ur} was increased from 1200 to 3000. Values of K of 1000 and K_{ur} of 3000 produced the most desirable results. This produced greatly reduced lateral movements during excavation and backfilling, and slightly reduced lateral movements during consolidation. No laboratory data was available to estimate K_{ur}, and K was originally estimated from staged CD tests, which are not ideal tests for determining modulus values. Confidence in the original K and K_{ur} values was not great, and the new values seem reasonable.

In order to produce a stiffer response during excavation and backfilling, the Poisson's ratio of the clay was reduced from 0.42 to 0.18. This greatly reduced lateral movements during excavation and backfilling, and slightly reduced lateral movements during con-

solidation. A Poisson's ratio of 0.18 seems to be a more realistic value for an overconsolidated clay than the original value of 0.42, which was estimated from laboratory tests. It appears that the method described in Section 4.3 to estimate Poisson's ratio from CU tests may not be a good method for heavily overconsolidated clays.

It was found that the amount of lateral movement that is predicted during backfilling is largely controlled by the initial effective vertical stress that is assumed for the soil-bentonite. If the initial effective vertical stress is increased from 40 to 100 psf, then less lateral deformation occurs during backfilling. It was thought that this increase in initial effective stress would also greatly decrease the amount of lateral deformation during consolidation; however, while it decreased lateral movements during backfilling by 50%, it only decreased lateral movements during consolidation by about 13%.

The R_f parameter value for sands was increased from 0.8 to 1.0 to soften the stiffness of the sand and possibly allow for more deformations during consolidation. This caused two beneficial results, a slight decrease in lateral movement during backfilling, and slight increase in lateral movement during consolidation.

Increasing the Young's modulus assumed for soil-bentonite during fill placement from 0.01 to 1.0 had little effect on lateral deformations. Increasing the compressibility of the soil-bentonite by increasing lambda increased the lateral movements only slightly during consolidation; however, it greatly increased the vertical settlement in the trench to unreasonable values. Increasing the value of lambda also resulted in unstable runs and crashing of the program due to excessive deformations in the trench. Values of lambda above 0.10 produced unreasonable settlements in the trench.

Removing the building load at 350 Ellis Street had virtually no effect on any lateral deformations. Therefore, any inaccuracies in the building load most likely had little effect.

Revised Analysis with Comparison with Measured Deformations

Changing some of the material properties of the existing sand and clay was successful in reducing the lateral movements during excavation and backfilling. The Poisson's ratio of the clay was changed from 0.42 to 0.18. The hyperbolic parameter, R_f, for the sand was changed from 0.8 to 1.0, and K_{ur} for the sand was changed from 1200 to 3000. Changing the initial effective stress of the soil-bentonite from 40 psf to 100 psf was successful in reducing lateral movements during backfilling without overly reducing lateral movements during consolidation. Using these modified procedures and parameters values, a modified analysis was run. The changes in the finite element model are summarized in Table 6.5.

Table 6.5 Modified Finite Element Analysis

Procedure or Parameter Value	Original Finite Element Model	Revised Finite Element Model
Initial Vertical Effective Stress for Soil-Bentonite	40 psf	100 psf
R_f Parameter for Sand	0.8	1.0
K_{ur} Parameter for Sand	1200	3000
Poisson's Ratio for Clay	0.42	0.18

The revised finite element model prediction of incremental lateral deformation is shown in Figure 6.19. It can be seen from the figure that the predicted and measured lateral deformations are within 1/4 inch for all phases of construction. The revised finite element model prediction of total settlement is shown in Figure 6.20. The figure shows that the model settlements are within 1/4 to 1/2 inch of the observed settlements for excavation and backfilling. The model is within 1/2 inch of most of the settlement points for consolidation. The revised finite element is well calibrated with the measured deformations. Since a successful calibration of the finite element model was achieved, the model was used to run a parametric study, which is described in Chapter 7.

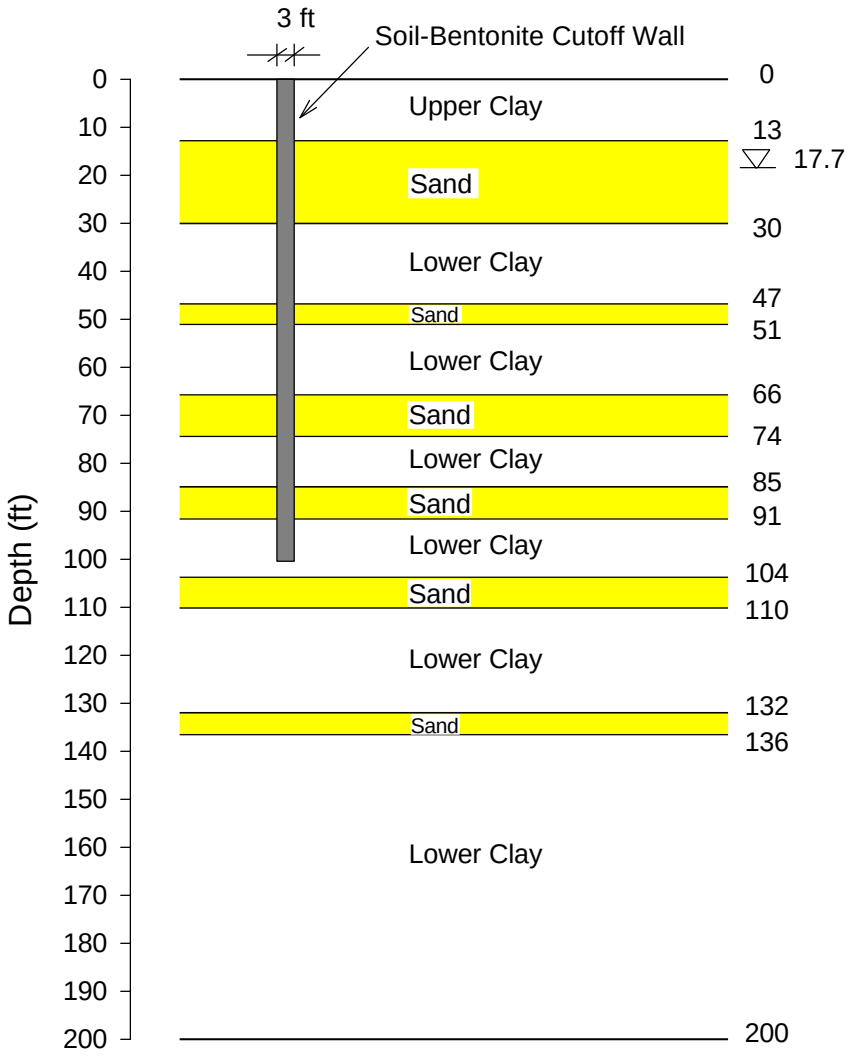

Figure 6.1 Soil Profile used in Finite Element Analyses

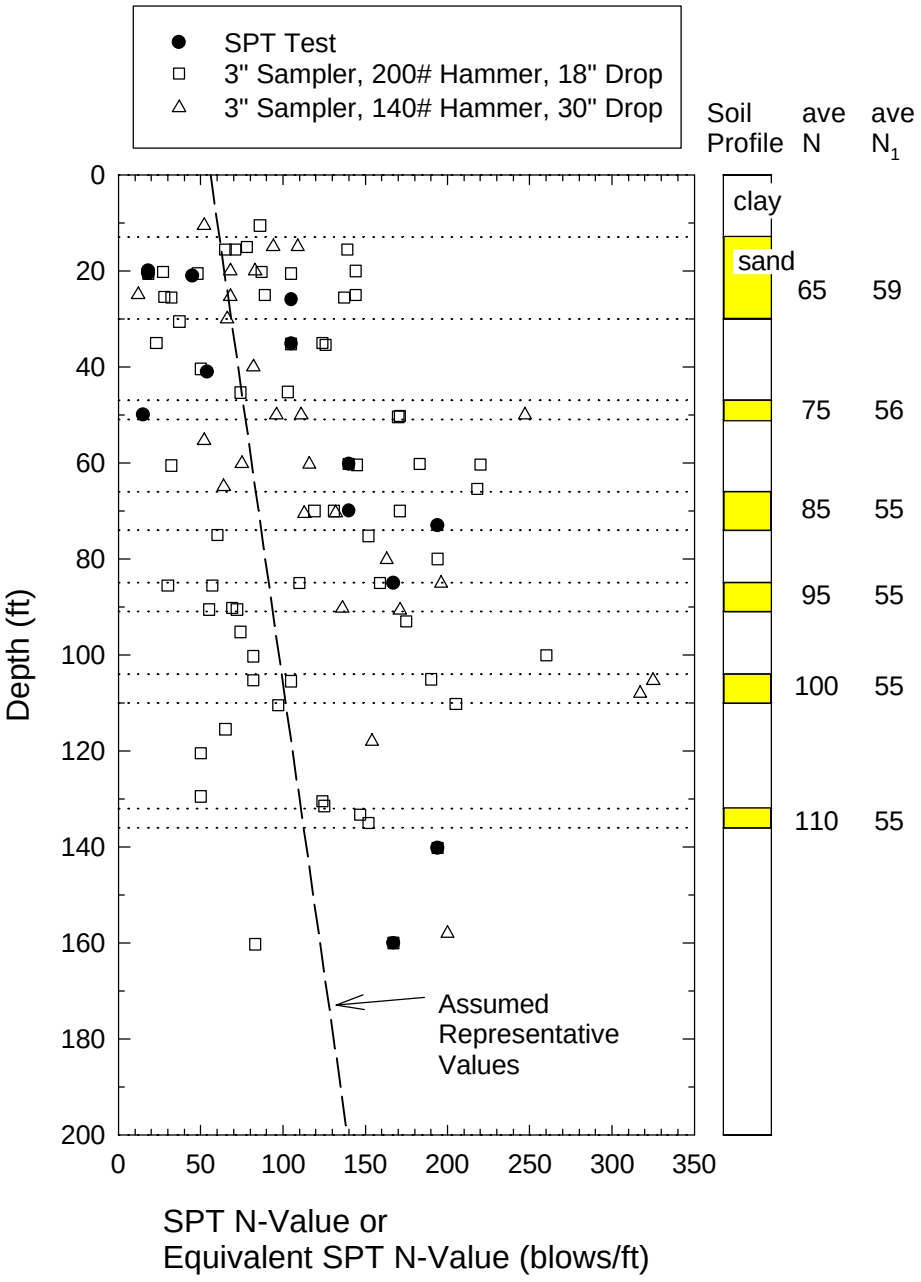

Figure 6.2 Penetration Tests Performed in Sand

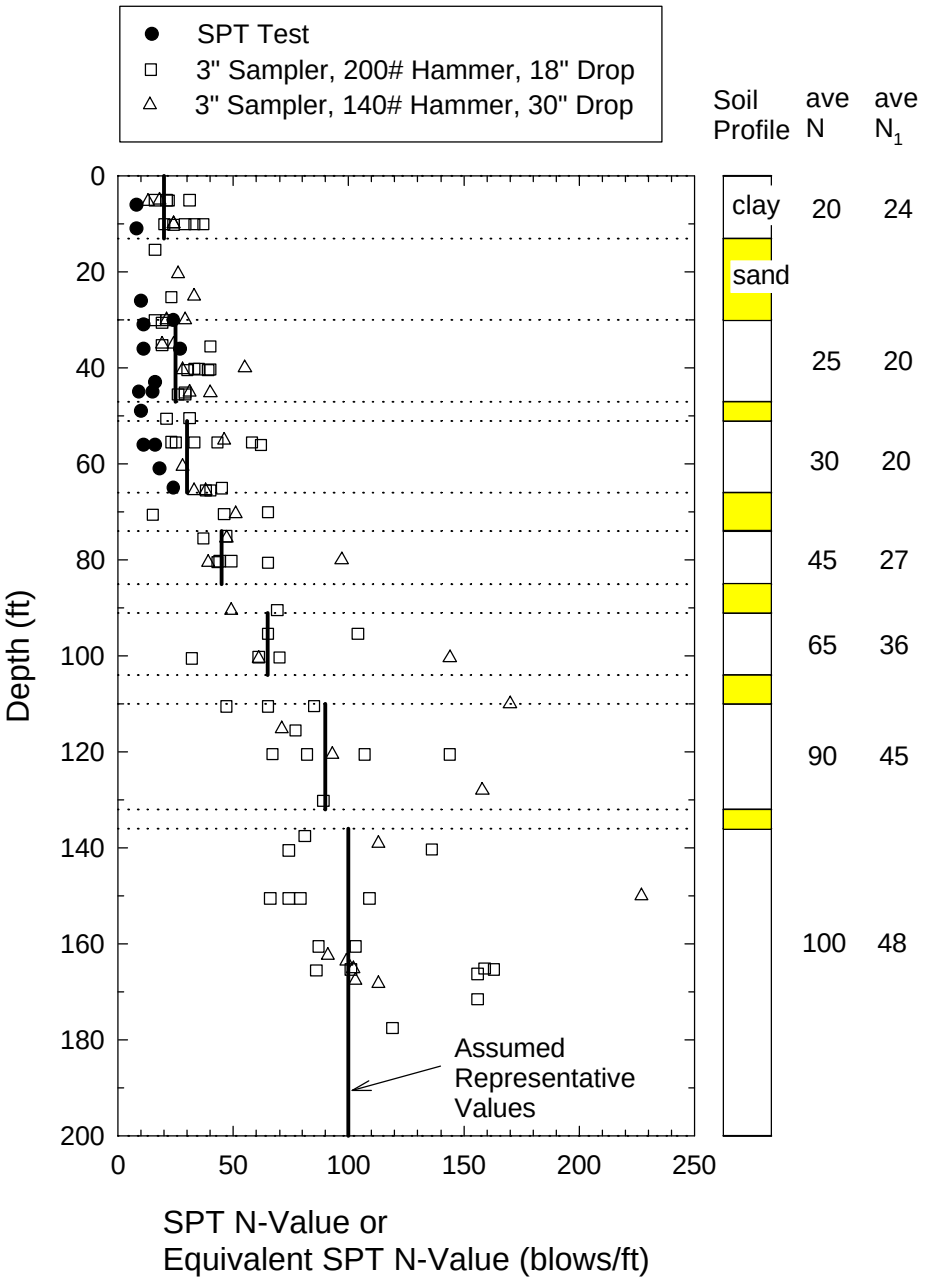

Figure 6.3 Penetration Tests Performed in Clays

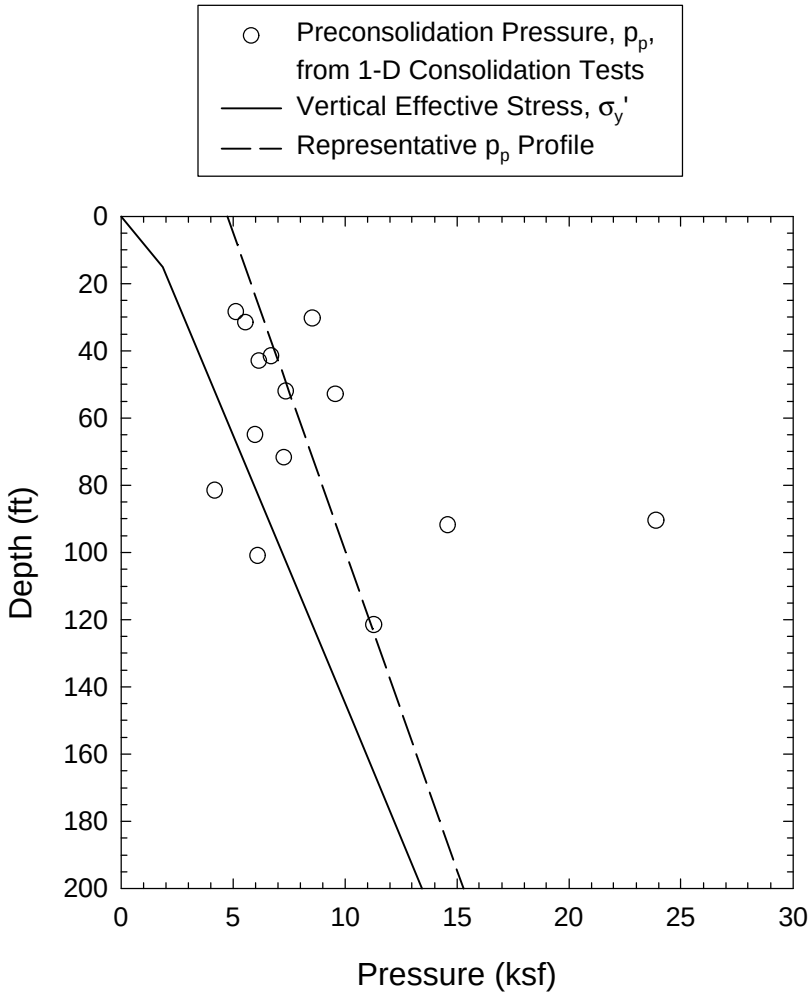

Figure 6.4 Preconsolidation Pressures from 1-D Consolidation Tests

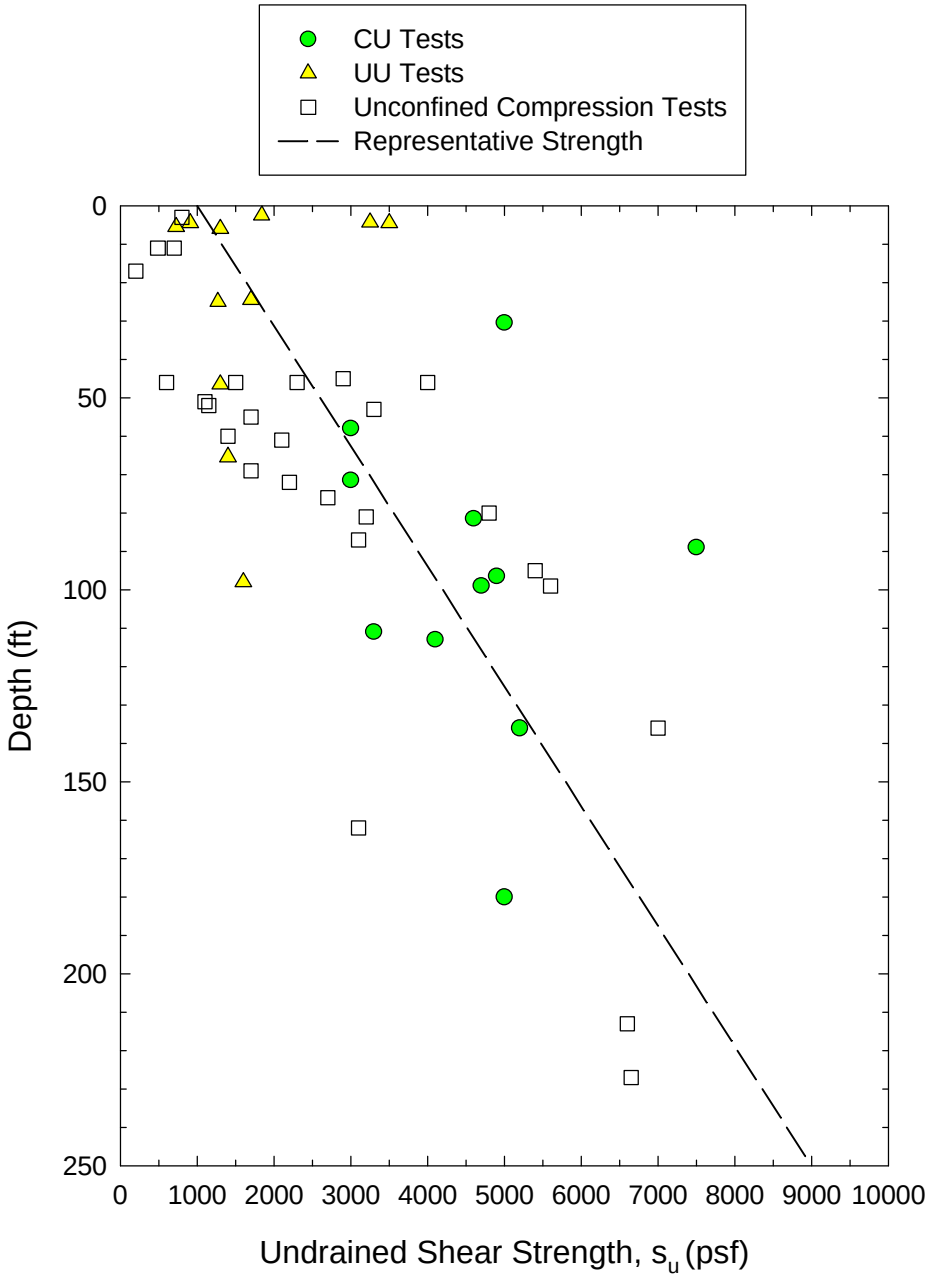

Figure 6.5 Undrained Shear Strengths for Clays

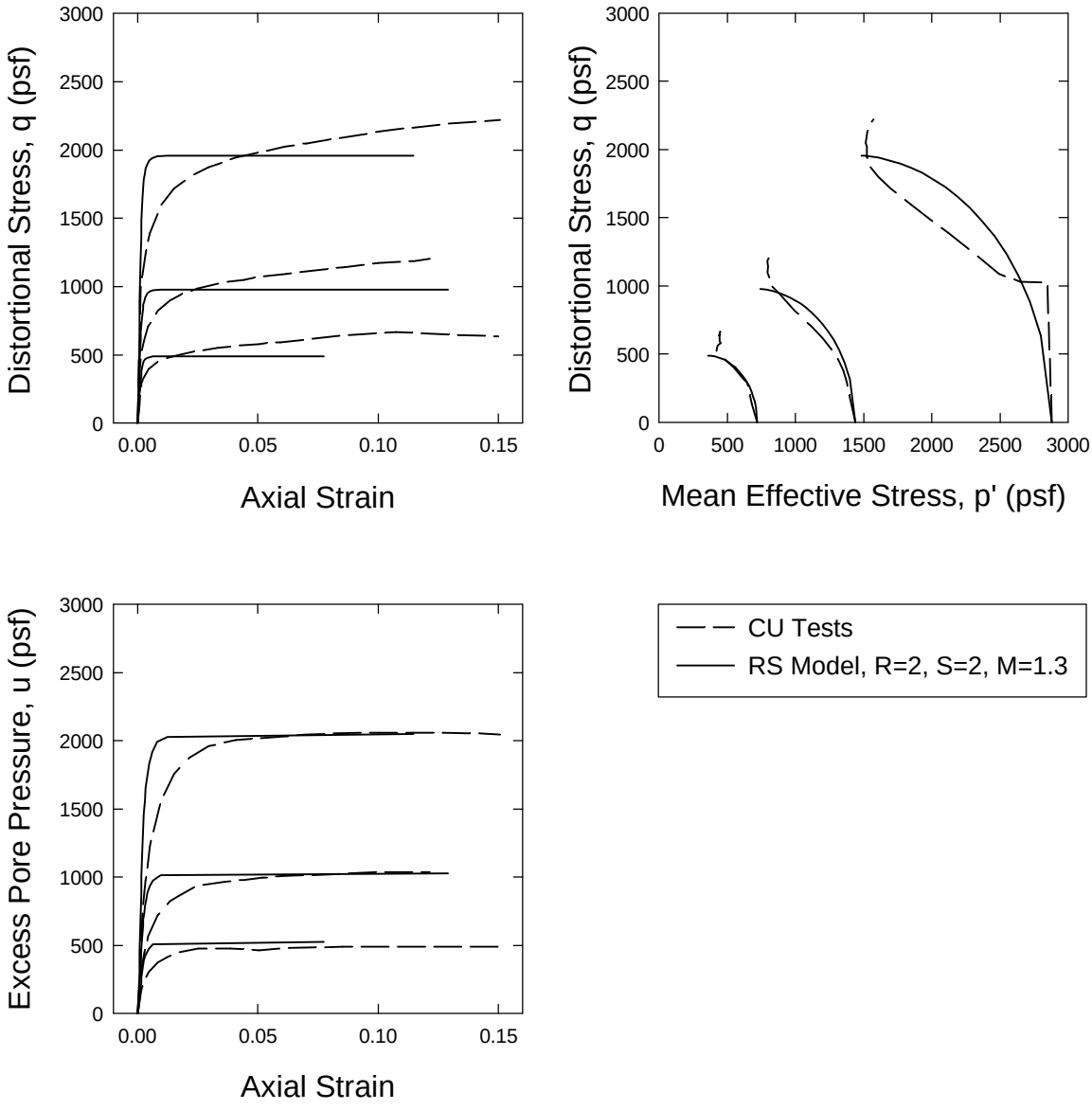

Figure 6.6 RS Model Predictions of CU Tests on Soil-Bentonite

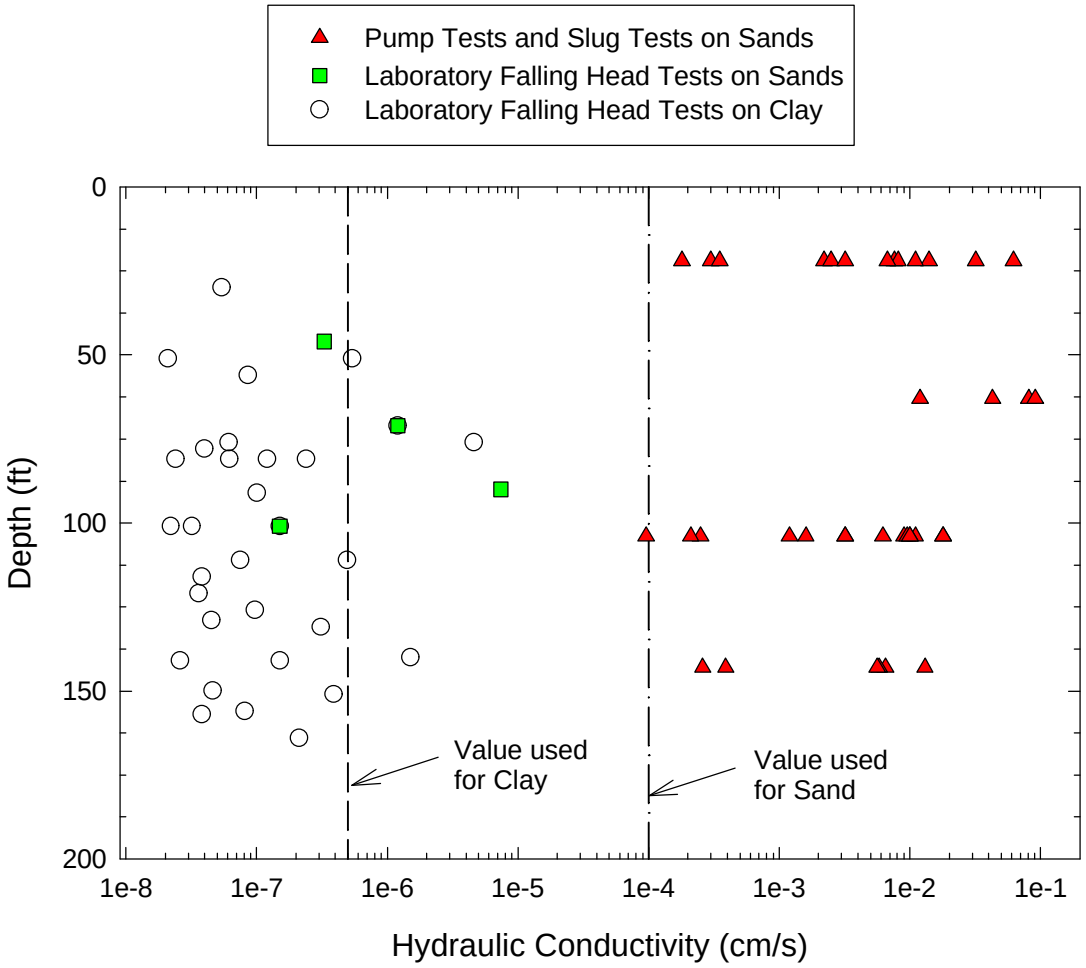

Figure 6.7 Hydraulic Conductivity Tests on Sands and Clays with Values used in Analyses

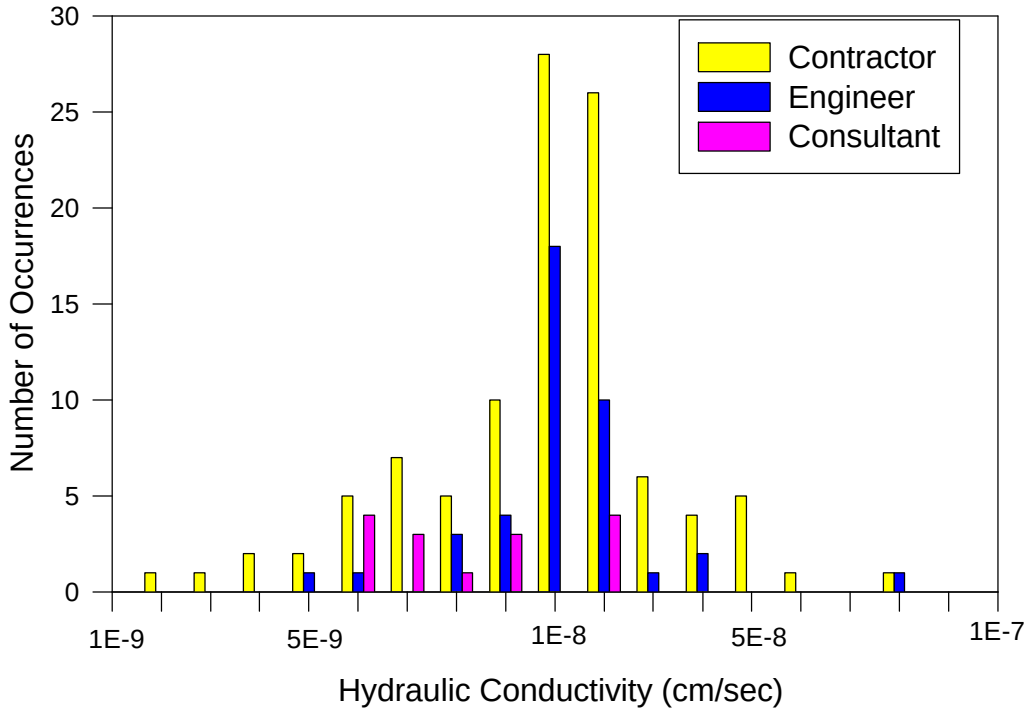

Figure 6.8 Hydraulic Conductivity Tests on Soil-Bentonite (after Burgess et al. 1988)

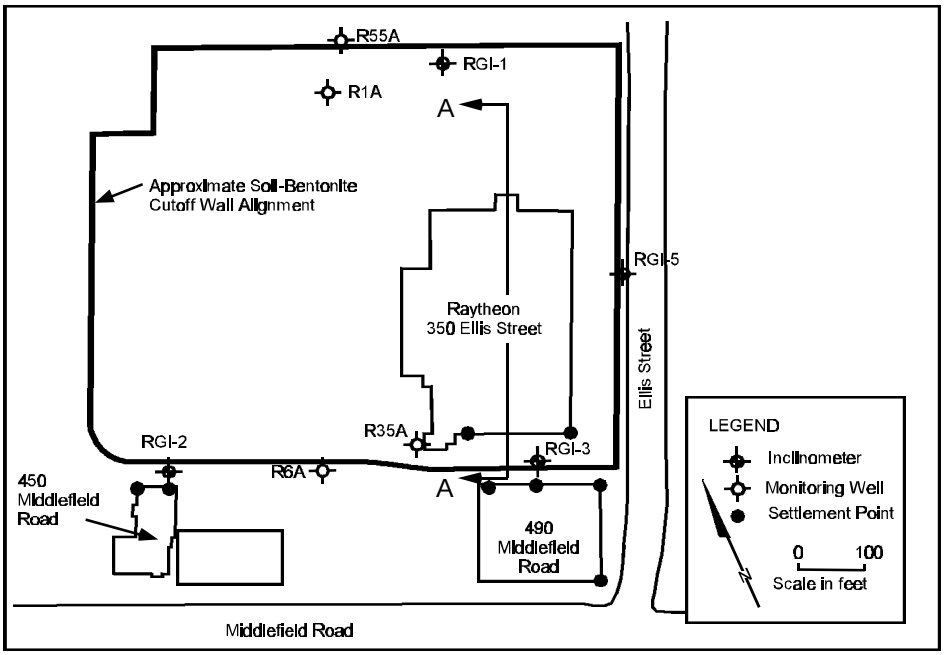

Plan

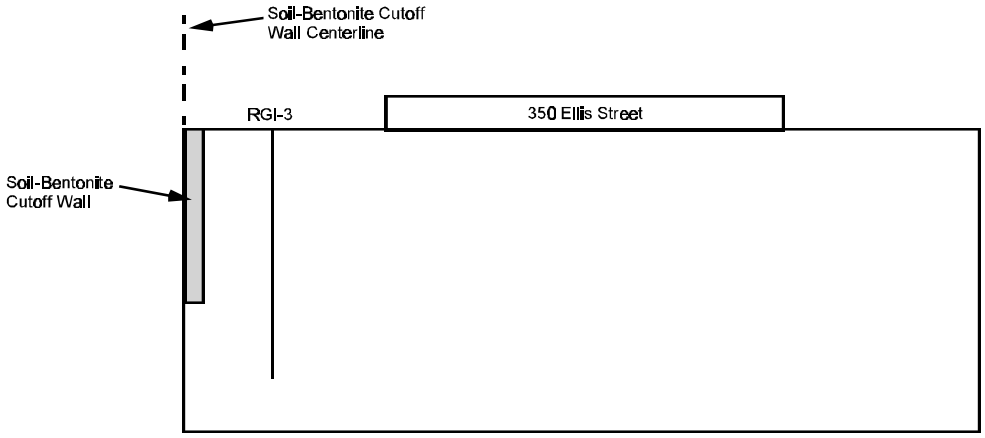

Section A-A
(Not to Scale)

Figure 6.9 Plan of Raytheon Site and Section Analyzed with Finite Element Model

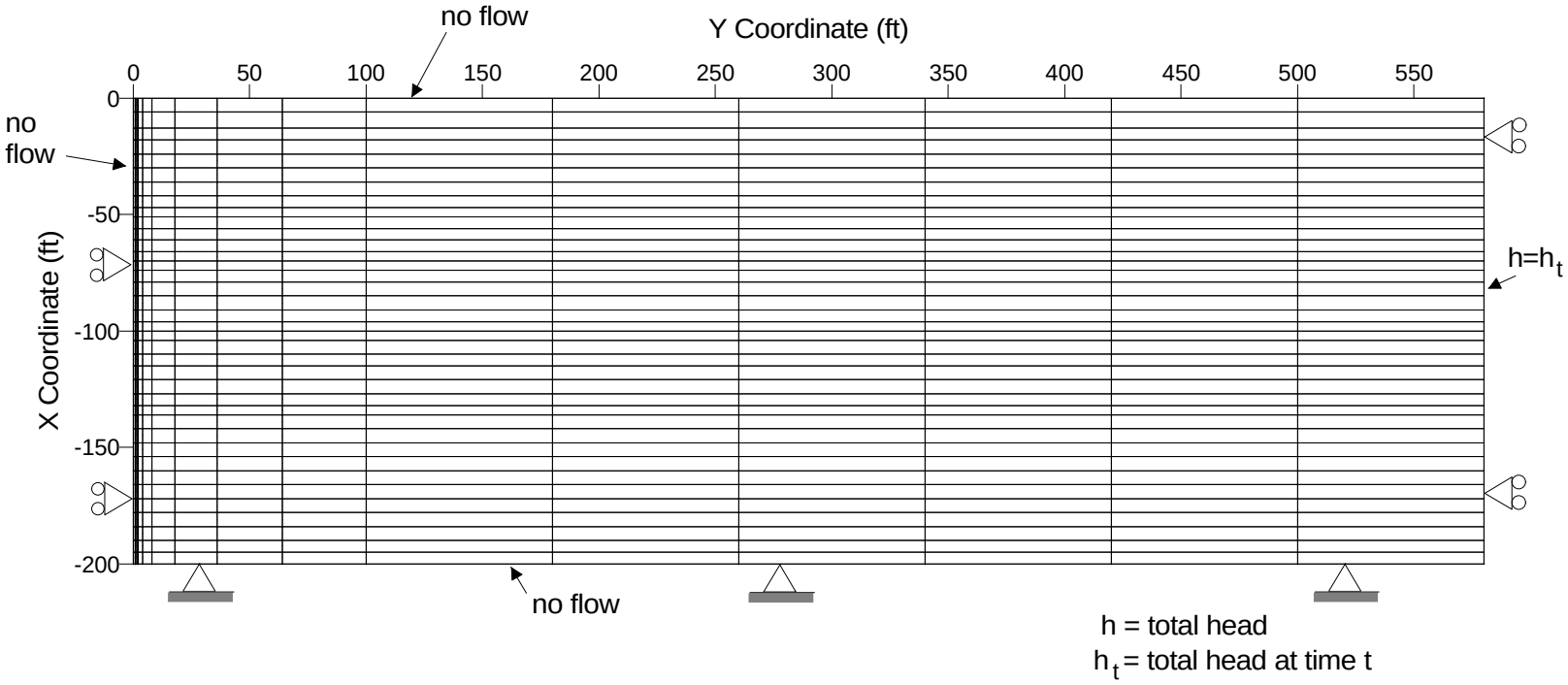

Figure 6.10 Finite Element Mesh and Boundary Conditions

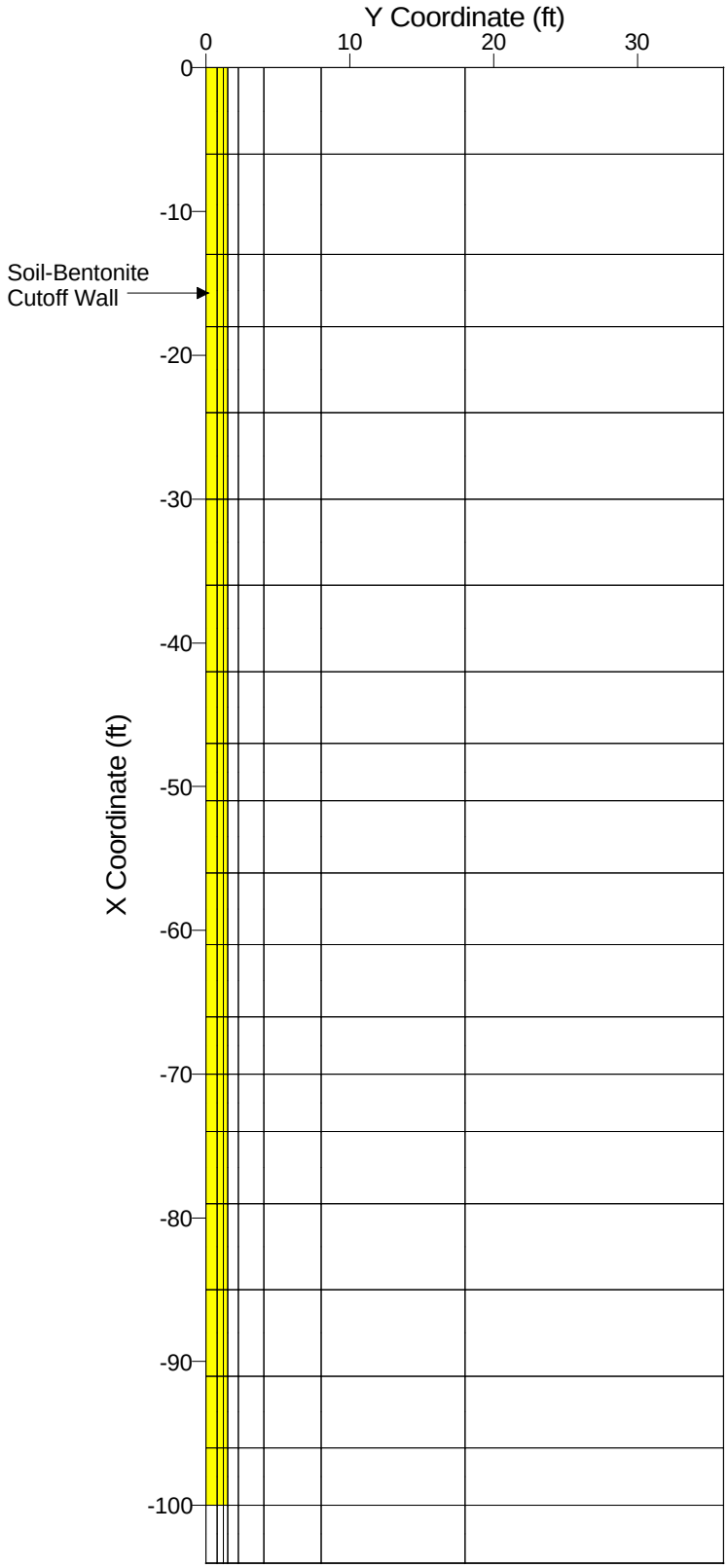

Figure 6.11 Enlargement of Finite Element Mesh Near Soil-Bentonite Cutoff Wall

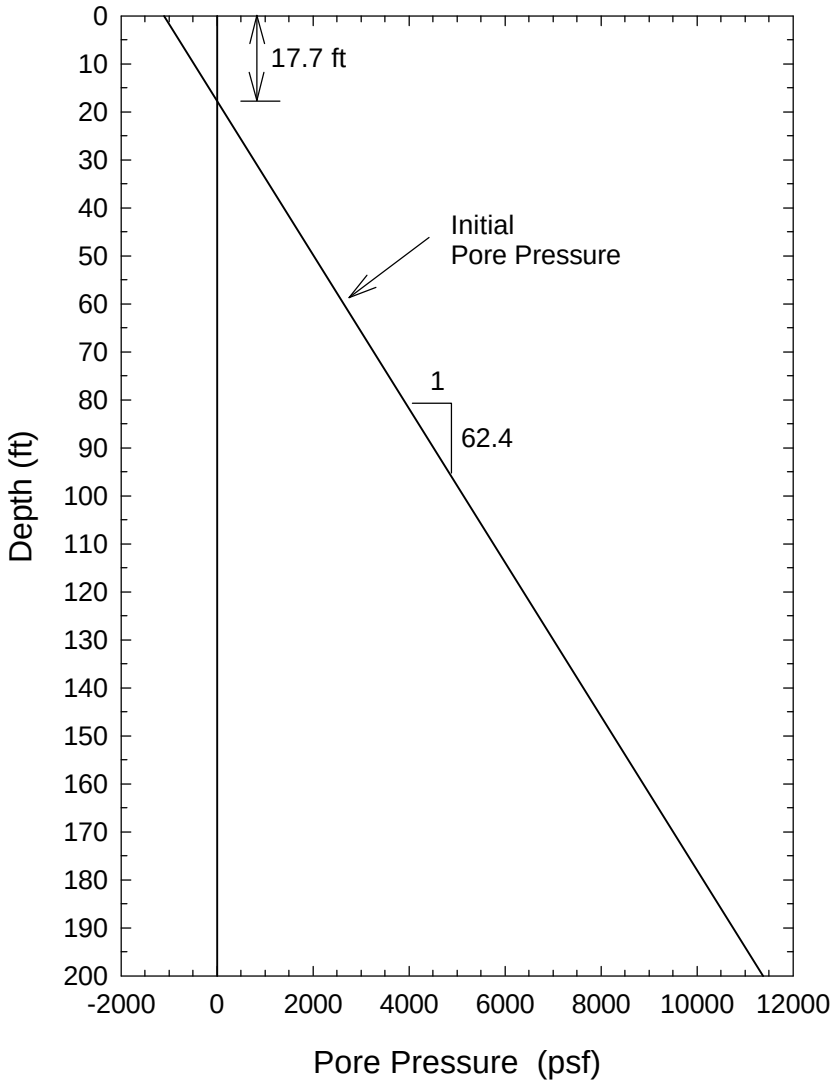

Figure 6.12 Assumed Initial Pore Pressures

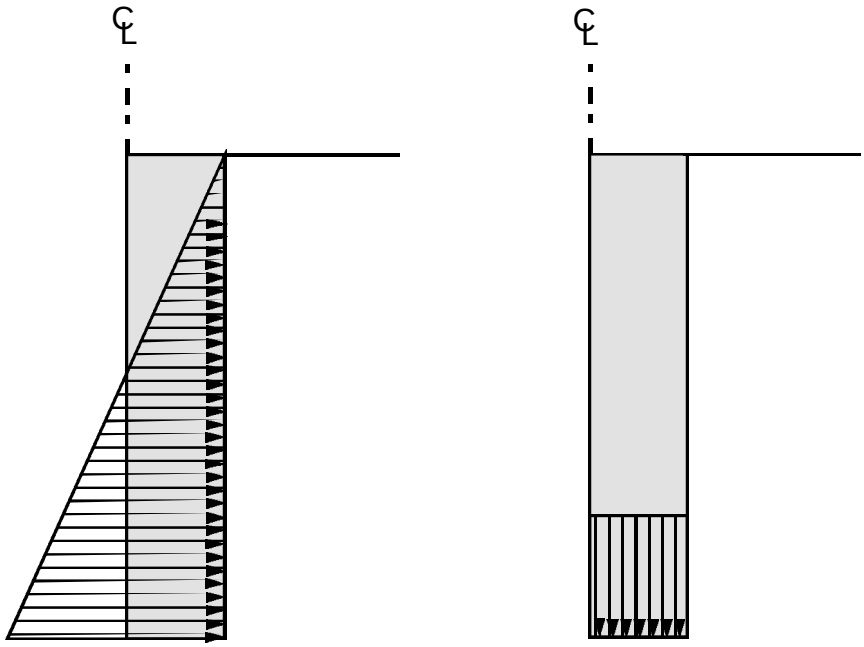

Figure 6.13 Stress Distributions Applied to Represent Bentonite-Water Slurry

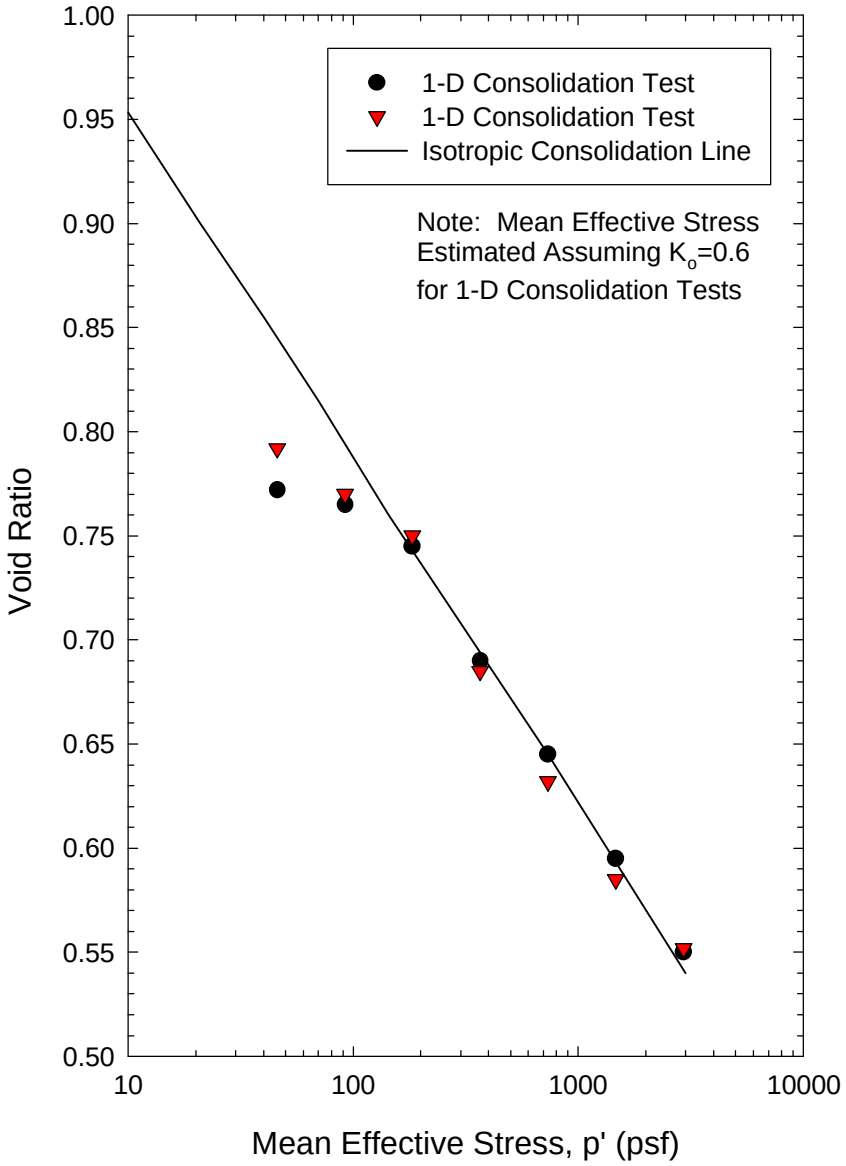

Figure 6.14 Void Ratio versus Mean Effective Stress for Soil-Bentonite

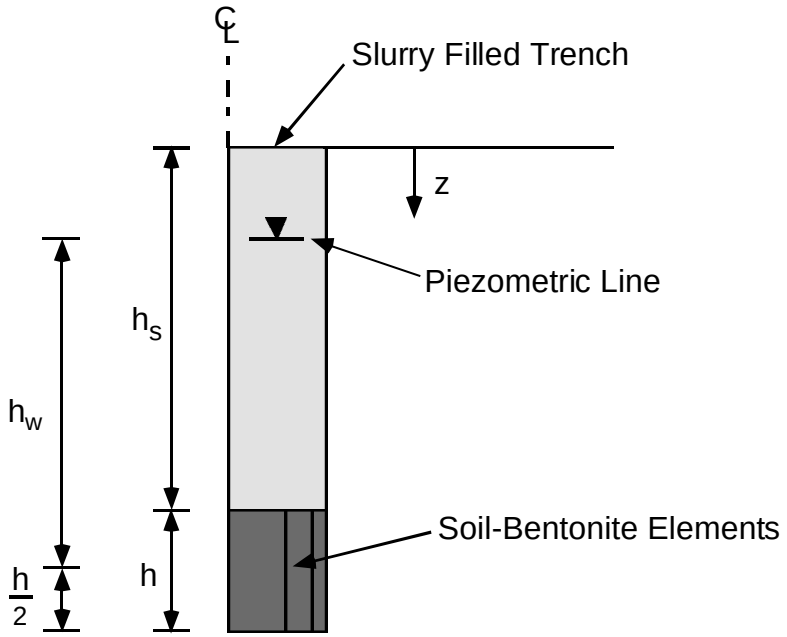

Figure 6.15 Schematic of Recently Placed Row of Soil-Bentonite Elements

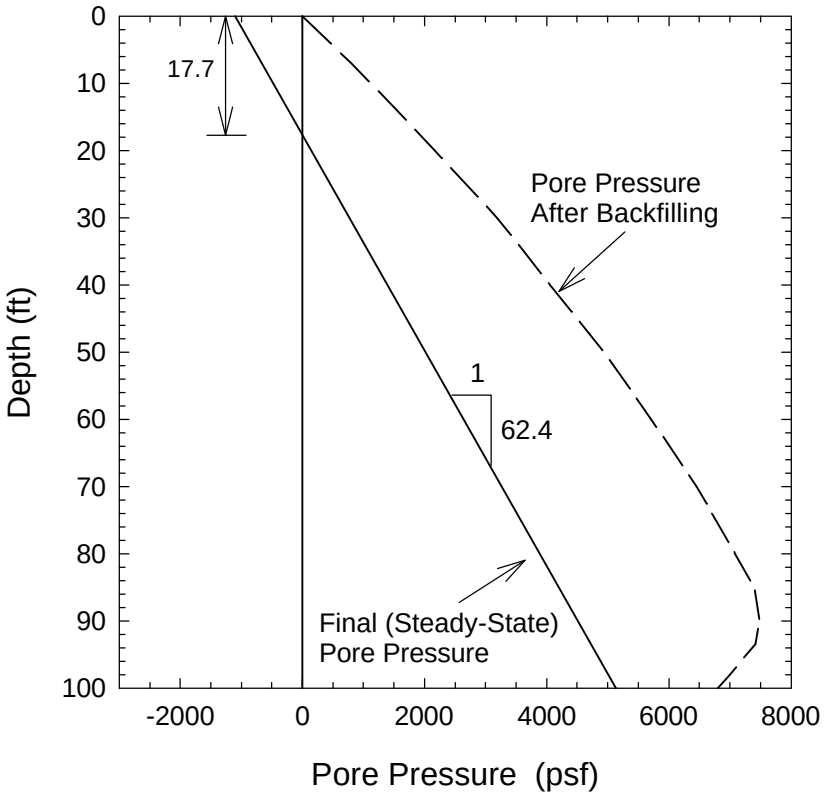

Figure 6.16 Pore Pressures in Soil-Bentonite Backfill

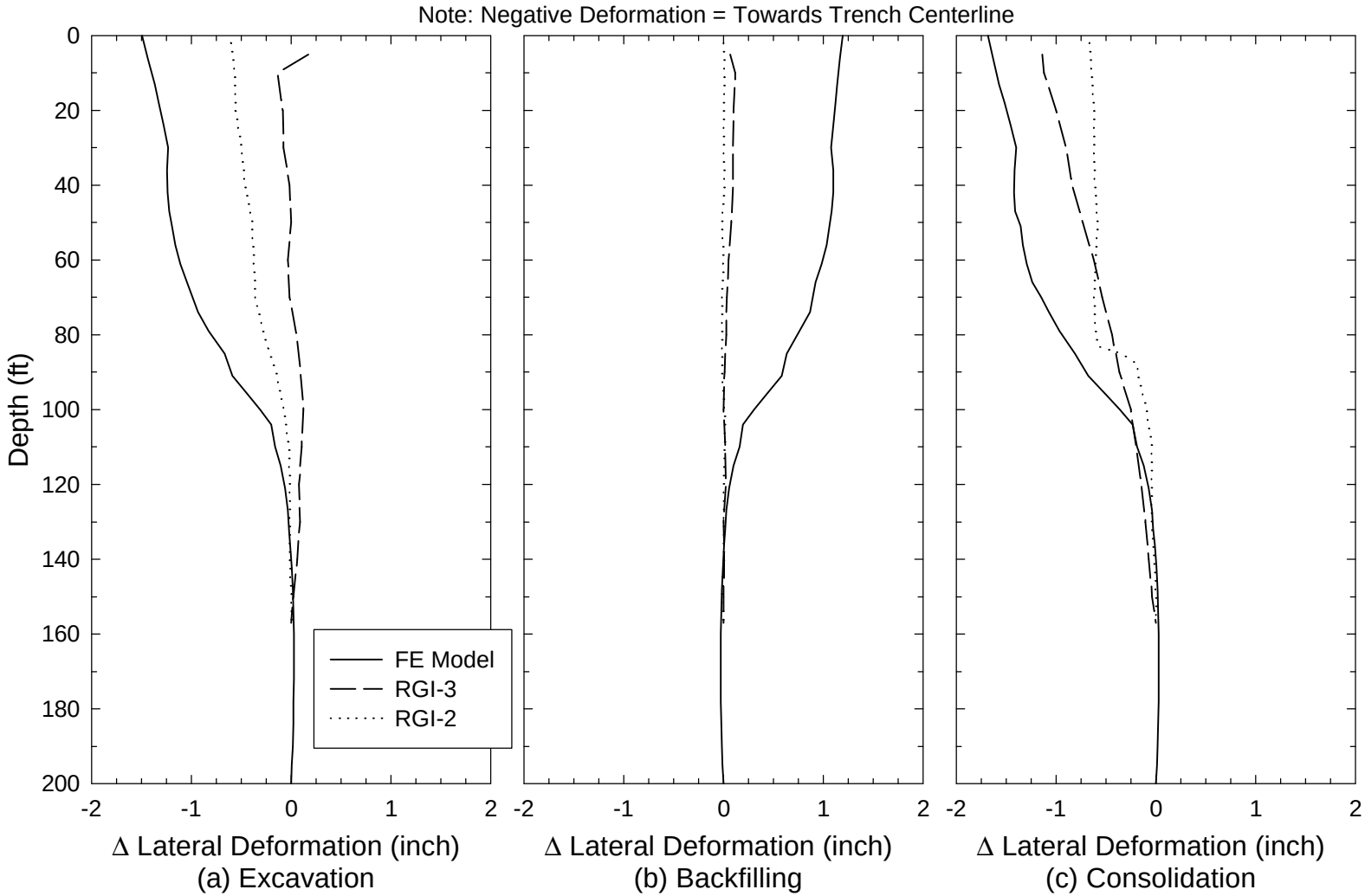

Figure 6.17 Comparison of Predicted and Measured Incremental Lateral Deformation

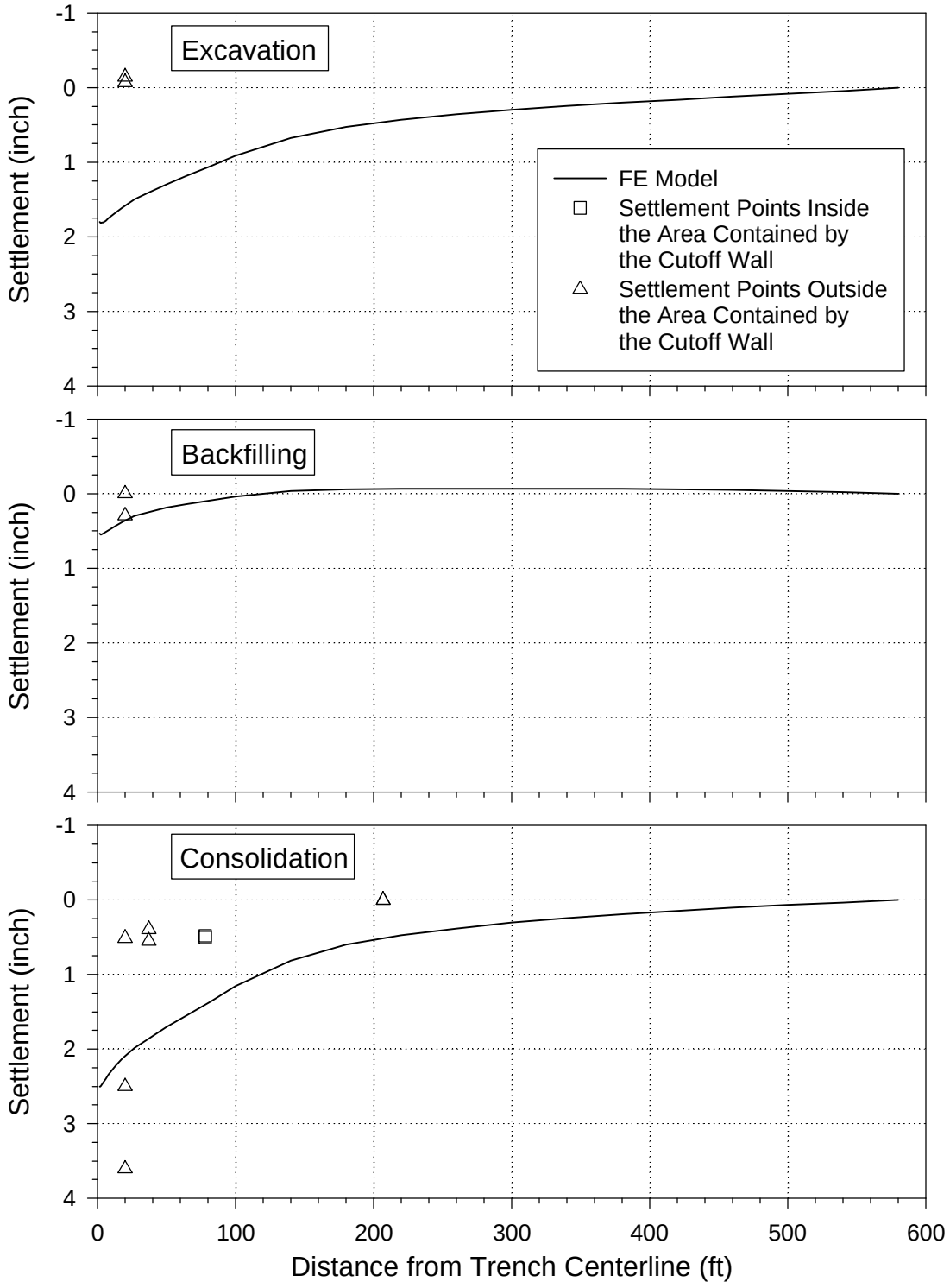

Figure 6.18 Comparison of Predicted and Measured Total Settlement of Ground Surface Adjacent to Soil-Bentonite Cutoff Wall

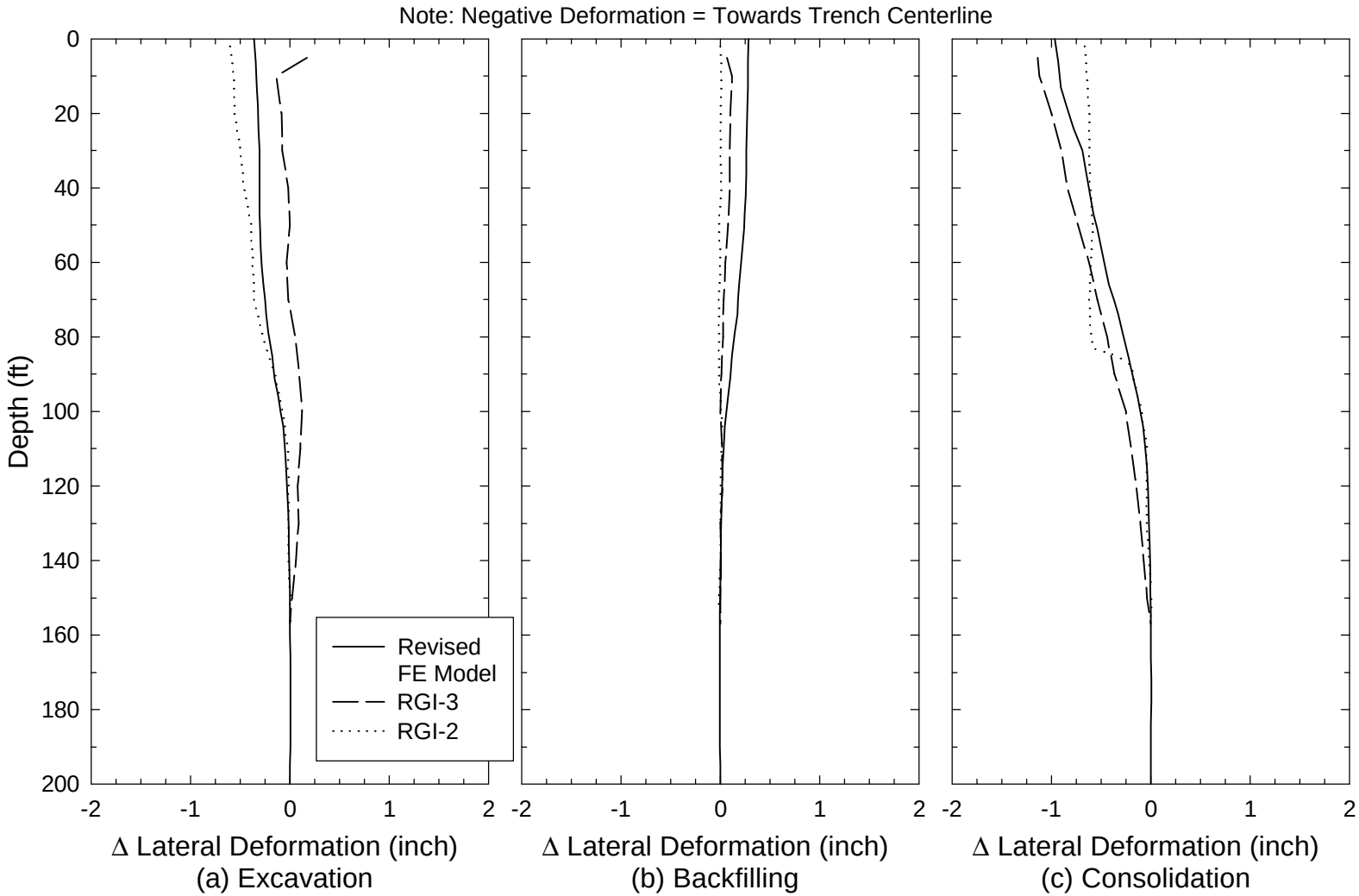

Figure 6.19 Revised Model: Predicted and Measured Incremental Lateral Deformation

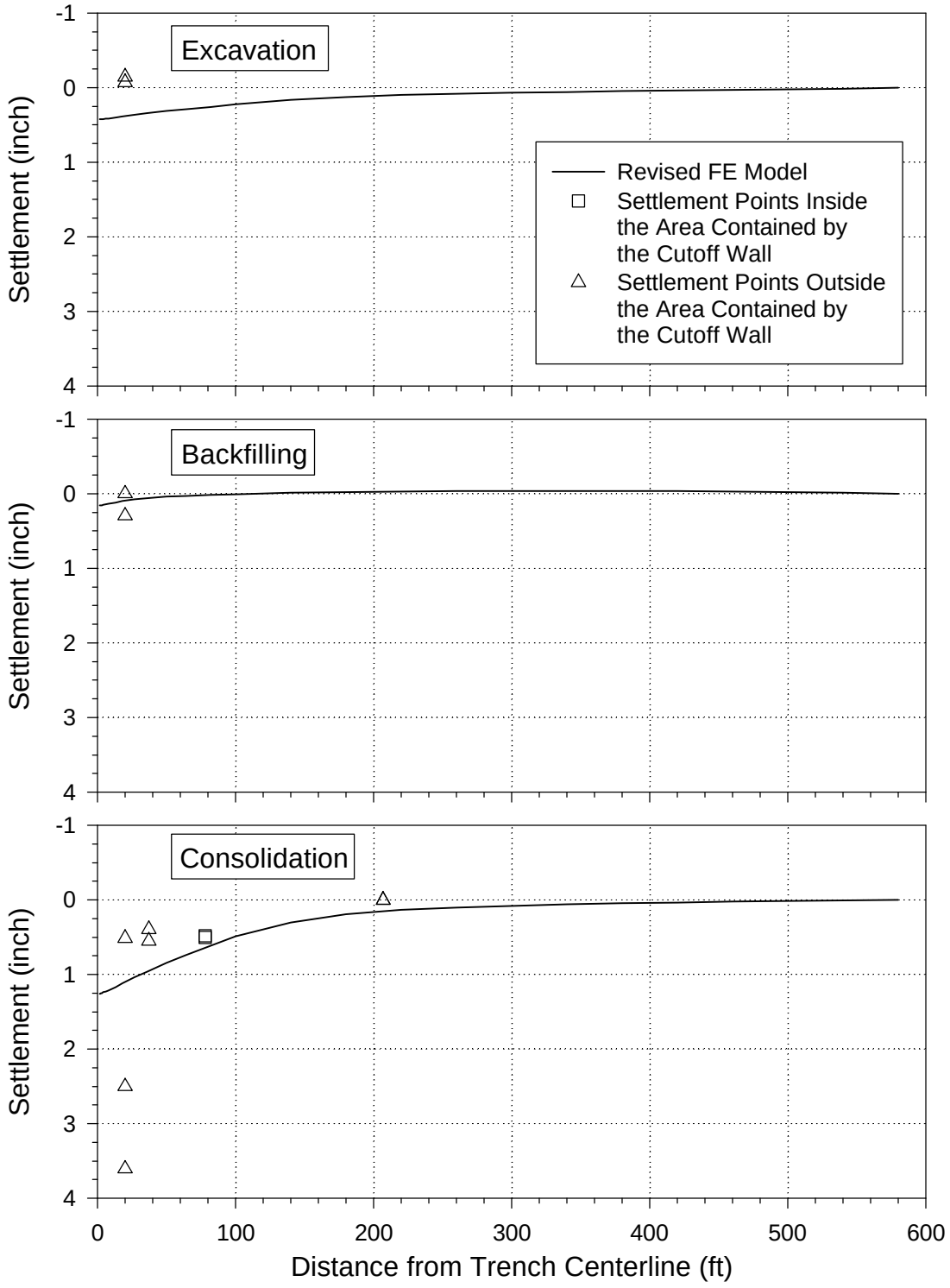

Figure 6.20 Revised Model: Predicted and Measured Total Settlement of Ground Surface Adjacent to Soil-Bentonite Cutoff Wall